Calibration of CORSIM Models under Saturated Traffic Flow Conditions

Final Report

September 2013

UNLV – TRC/UTC

Prepared for

NEVADA DEPARTMENT OF TRANSPORTATION AND

UNIVERSITY TRANSPORTATION RESEARCH CENTER

Prepared By

Alexander Paz Ph.D., P.E.

Assistant Professor
Department of Civil and Environmental Engineering
University Transportation Center – Transportation Research Center
University of Nevada Las Vegas
4505 S Maryland Parkway, Las Vegas
Nevada – 89154
Ph. No: (702) 895-0571
Email: apaz@unlv.edu

and
Victor Hugo Molano-Paz, M.S.

Ph.D. Student
Department of Civil and Environmental Engineering
University Transportation Center – Transportation Research Center
University of Nevada Las Vegas
4505 S Maryland Parkway, Las Vegas
Nevada 89154
Victor.hugo.molano@gmail.com

UNLV | Howard R. Hughes College of ENGINEERING

TECHNICAL REPORT DOCUMENTATION PAGE

Report No.	2. Government Accession No.	3. Recipients Catalog No.
4. Title and Subtitle Calibration of CORSIM Models under Saturated Traffic Flow Conditions		5. Report Date September 2013
6. Performing Organization Code		
7. Author(s) Alexander Paz, Victor Hugo Molano Paz		8. Performing Organization Report No.
9. Performing Organization Name and Address University of Nevada Las Vegas 4505 S Maryland Parkway, BOX 404505 Las Vegas, NV 89154		10. Work Unit No.
11. Contract or Grant No.		
12. Sponsoring Agency Name and Address **Nevada Department of Transportation and the University Transportation Research Center**		13. Type or Report and Period Covered
14. Sponsoring Agency Code **NDOT & UTC**		
15. Supplementary Notes		

16. Abstract

This study proposes a methodology to calibrate microscopic traffic flow simulation models. The proposed methodology has the capability to calibrate simultaneously all the calibration parameters as well as demand patterns for any network topology. These parameters include global and local parameters as well as driver behavior and vehicle performance parameters; all based on multiple performance measures, such as link counts and speeds. Demand patterns are included in the calibration framework in terms of turning volumes. A Simultaneous Perturbation Stochastic Approximation (SPSA) algorithm is proposed to search for the vector of the model's parameters that minimizes the difference between actual and simulated network states. Previous studies proposed similar methodologies; however, only a small number of calibration parameters were considered, and none of the demand values. Moreover, an extensive and *a priori* process was used in order to choose the subset of parameters with the most potential impact.

In the proposed methodology, the simultaneous consideration of all model parameters and multiple performance measures enables the determination of better estimates at a lower cost in terms of a user's effort. Issues associated with convergence and stability are reduced because the effects of changing parameters are taken into consideration to adjust them slightly and simultaneously. The simultaneous adjustment of all parameters results in a small number of evaluations of the objective function. The experimental results illustrate the effectiveness and validity of this proposed methodology. Three networks were calibrated with excellent results. The first network was an arterial network with link counts and speeds used as performance measurements for calibration. The second network included a combination of freeway ramps and arterials, with link counts used as performance measurements.

Considering simultaneously arterials and freeways is a significant challenge because the two models are different and their parameters are calibrated at the same time. This represents a higher number of parameters, which increases the complexity of the optimization problem. A proper solution from all feasible solutions becomes harder to find. The third network was an arterial network, with time-dependent link counts and speed used as performance measurements. The same set of calibration parameters was used in all experiments. All calibration parameters were constrained within reasonable boundaries. Hence, the design and implementation of the proposed methodology enables the calibration of generalized micro-simulation traffic flow simulation models.

17. Key Words	18. Distribution Statement
Microscopic Traffic Flow, Simulation Models, Calibration Parameters, Demand Patterns, Driver Behavior	**Unrestricted. This document is available through the National Technical Information Service, Springfield, VA 21161**

19. Security Classif is report)	20. Security Classif. (of this page)	21. No. Of Pages	22. Price
Unclassified	**Unclassified**		

ACKNOWLEDGEMENTS

The authors acknowledge the assistance of several individuals who supported the work described in this research report. These individuals include: faculty members from UNLV's College of Engineering as well as Carlos Gaviria and Christian Arteaga for their help and support during the development of the implementation component of this study. Funding to support this research was provided by the Nevada Department of Transportation, the Regional Transportation Commission Southern Nevada, the University of Nevada at Las Vegas (UNLV), and the UNLV University Transportation Center.

DISCLAIMER

The opinions, findings, and conclusions expressed in this publication are those of the authors and not necessarily those of the Nevada Department of Transportation or University of Nevada, Las Vegas. Alternative accessible formats of this document will be provided upon request. Persons with disabilities who need an alternative accessible format of this information, or who require some other reasonable accommodation to participate, should contact Dr. Alexander Paz, Assistant Professor, Department of Civil and Environmental Engineering, University of Nevada, Las Vegas. Tel: (702) 895-0571; cell: (702) 688-3878; E-mail: apaz@unlv.edu.

TABLE OF CONTENTS

LIST OF TABLES

LIST OF FIGURES

CHAPTER 1 INTRODUCTION

Micro-simulation models provide tremendous capabilities to model, at a high level of resolution, complex systems in a broad range of fields, including economy, sociology, physics, chemistry, and engineering (Anderson & Hicks, 2011). In the context of vehicular traffic systems, microscopic traffic flow models enable the modeling of many aspects of the actual system, including the maneuvers of individual vehicles and their interactions, the various types and characteristics of facilities, and the vast number of control settings. These capabilities are associated with a large number of modeling parameters that typically need to be tailored for each vehicular system. For example, driver behavior includes parameters associated with car following, lane-changing maneuvers, and gap acceptance. Thus, the quality of the model and the validity of its results are highly dependent on the correctness of the chosen parameters (Breski, Cvitanic, & Lovric, 2006; Brockfeld, Kuhne, & Wagner, 2005; Holm, Tomich, Sloboden, & Lowrance, 2007; Kim & Rilett, 2003; Kondyli, Soria, Duret, & Elefteriadou, 2012; Schultz & Rilett, 2004; Schultz & Rilett, 2005). Hence, it is important to consider all these model parameters simultaneously with the aim to capture their *intricate* effects, thereby enabling convergence and stability of the solutions (see Appendix A).

A broad number of optimization algorithms, ranging from genetic algorithms to finite difference stochastic approximation, can be used to determine an adequate set of model parameters for a particular traffic system (Breski et al., 2006; Brockfeld et al., 2005; Cunha, Bessa Jr., & Setti, 2009; Kim & Rilett, 2003; Toledo, Ben-Akiva, Darda, Jha, & Koutsopoulos, 2004). For example, the sequential simplex algorithm has been used to calibrate parameters for car-following, acceleration/deceleration, and lane-

changing behavior(Kim & Rilett, 2003). However, only a subset of parameters was considered. Moreover, parameters associated with infrastructure and vehicle performance were not considered. The algorithm provided adequate results under congested conditions. However, under low-congestion conditions, manual calibration provided better results.

Genetic Algorithms (GA) were used for the calibration of global and local capacity and occupancy parameters (Jha et al., 2004; Ma, Dong, & Zhang, 2007). A sequential approach was used to update global and local parameters. Simultaneous Perturbation Stochastic Approximation (SPSA) algorithms also have been proposed. J. Lee used SPSA algorithms to calibrate model parameters and demand patterns, using various stages(Lee, 2008). The calibration capabilities of GA and SPSA algorithms were shown to be similar; however, SPSA algorithms were less computationally intensive (Ma et al., 2007). In addition, SPSA and Finite Difference Stochastic Approximation algorithms have been proposed for the calibration of demand and supply parameters (Balakrishna, Antoniou, Ben-Akiva, Koutsopoulos, & Wen, 2007). However, driver behavior parameters were pre-calibrated, and the calibration was based only on link sensor counts. Other important performance measures, such as speed, were not considered. Previous studies did not simultaneously calibrate all model parameters while concurrently considering multiple performance measures, such as link counts and speed.

This study seeks to develop a methodology to calibrate simultaneously all model parameters and demand patterns based on link counts and speeds. This is in contrast with previous studies in which either only a subset of model parameters were considered, a single performance measure was used, or demand patterns were pre-calibrated. The

proposed methodology uses a SPSA algorithm to determine an adequate set of all model parameters and turning volumes.

The SPSA was chosen based on its computationally efficiency and ability to handle large numbers of parameters (Balakrishna et al., 2007; Chin, 1997; Lee, 2008; Maryak & Spall, 2005; Spall, 1998a; Spall, 2003; Spall, 1995; Spall, 1998b). Only two traffic flow simulation evaluations per iteration of the SPSA are required to update all model parameters. Running a low number of traffic flow simulations represents important savings in terms of time and other resources. Comparative studies between SPSA and other algorithms could be found in the literature (Balakrishna et al., 2007; Chin, 1997; Spall, 2003). In addition, the SPSA algorithm was used to calibrate and optimize various transportation applications (Lee, 2008; Lee & Ozbay, 2009; Ma et al., 2007).

CHAPTER 2 METHODOLOGY

Formulation of the Calibration Problem

The calibration problem for all model parameters, θ, is formulated using a mathematical programming approach. The analysis period is divided into a number *T* of discrete time periods. The objective function, normalized root mean square (*NRMS*), as denoted by Equation (2.1), is the sum over all calibration time-periods of the average of the sum over all links *I* of the root square of the square of the normalized differences between actual and simulated link counts and speeds. The normalization enables the consideration of multiple performance measures, in this case, link counts and speeds. The calibration problem is formulated as follows:

Minimize *NRMS* =

$$\frac{1}{\sqrt{n}} * \sum_{t=1}^{T} (W * \sqrt{(\sum_{i=1}^{n} (\frac{V_i - \tilde{V}(\theta)_i}{V_i})^2)} + (1-W) * \sqrt{\sum_{i=1}^{n} (\frac{S_i - \tilde{S}(\theta)}{S_i})^2}) \qquad (2.1)$$

subject to:

Lower bound $\leq \theta \leq$ Upper bound

where:

V_i = actual link counts for link *i*

$\tilde{V}(\theta)_i$ = simulated link counts for link *i*

S_i = actual speeds for link *i*

$\tilde{S}(\theta)$ = simulated speeds for link *i*

n= total number of links in the model

T = total number of time periods

W = weight used to assign more or less value to counts or speeds

Calibration criteria

The calibration criteria for this study were based on guidelines from the Federal Highway Administration, as summarized in Table 1.

Table 1. Calibration Guidelines for Simulation Models of Microscopic Traffic Flow

Traffic Volumes	Difference between actual and simulated link counts	< 5%	For all links
	GEH statistic	< 5	For at least 85% of the links

where:

$$GEH = \sqrt{\frac{2(V_i - \tilde{V}(\theta)_i)^2}{V_i + \tilde{V}(\theta)_i}} \qquad (2.2)$$

V_i = actual link counts at the link i

$\tilde{V}(\theta)_i$ =simulated link counts at the link i

Simultaneous Perturbation Stochastic Approximation algorithm

The SPSA algorithm is an iterative approach that uses gradient estimations of the objective function to determine an optimal solution. Details of its implementation are provided by James C. Spall (Spall, 1998a; Spall, 2003; Spall, 1995; Spall, 1998b).

Characteristics of the SPSA Algorithm

In each iteration of SPSA, the vector of model parameters is updated using Equation (2.3):

$$\theta_{k+1} = \theta_k - a_k g_k \theta_k \tag{2.3}$$

where,

θ_{k+1} = vector of updated parameters at iteration k+1

θ_k= vector of initial parameters at iteration k+1

a_k=gain coefficient at iteration k+1 calculated using Equation (2.4)

$g_k\theta_k$= estimated gradient at iteration k+1.

$$a_k = \frac{a}{(k+1+A)^{\alpha}} \tag{2.4}$$

where$a$, A, and α are empirical non-negative coefficients. These coefficients affect the convergence of the SPSA algorithm.

The simultaneous perturbation and gradient estimate are represented by $g_k\theta_k$, and is calculated using Equation (2.5):

$$g_k\theta_k = \frac{y(\theta_k+c_k\Delta_k)-y(\theta_k-c_k\Delta_k)}{2ck}\left[\Delta_{k1}^{-1}, \Delta_{k2}^{-1}, \Delta_{k3}^{-1}, \dots, \Delta_{kp}^{-1}\right]^T \tag{2.5}$$

Here, c_k is calculated using Equation (2.6), where c and Υ are empirical non-negative coefficients:

$$c_k = \frac{c}{(k+1)^{\Upsilon}} \tag{2.6}$$

The elements in the random perturbation vector $\Delta_k = \left[\Delta_{k1}^{-1}, \Delta_{k2}^{-1}, \Delta_{k3}^{-1}, \dots, \Delta_{kp}^{-1}\right]^T$ are Bernoulli-distributed, with a probability of one-half for each of the two possible outcomes.

Algorithmic Steps

The SPSA algorithm is implemented using the following steps (Spall, 2003):

Step 1: Set counter *k* equal to zero. Initialize coefficients for the gain function *a*, *A*, and α and calibration parametersθ_0.

Step 2: Generate the random perturbation, vector Δ_k.

Step 3: Evaluate the objective function, plus and minus the perturbation.

Step 4: Evaluate the gradient approximation $g_k\theta_k$.

Step 5: Update the vector of calibration parameters using Equation (2.3) along with the corresponding constraints denoted by Equation (1).

Step 6: Check for convergence. If convergence is achieved, stop; otherwise, set counter $k = k + 1$ and repeat Steps 1-6.

Convergence of the calibration

Convergence is reached when the inequality in Equation (2.9) is satisfied or a user pre-specified maximum number of iterations is reached. At convergence, the calibration criteria are expected to be satisfied or a significantly better model is obtained.

$$\frac{\sum_{k-N}^{k}\sqrt{(NRMS_{AV}-NRMS_k)^2}}{N} < \rho \qquad (2.9)$$

where,

$NRMS_{AV}$= average *NRMS* of the last *k-N* iterations

$NRMS_k$= *NRMS* at k iteration

k= iteration counter

N= pre-specified integer

ρ = pre-specified convergence condition

CHAPTER 3 SOFTWARE IMPLEMENTATION

A software tool was developed to implement the proposed calibration methodology. It was developed using a basic layered architecture were each layer handles a group of related functions. The tool contains four different layers: (i) a Graphical User Interface (GUI); (ii) a Domain; (iii) a Persistence; and (iv) a Facade. The GUI enables the user to interact with the entire software tools. It provides a user-friendly mechanism to create and edit calibration workspaces. The Domain performs all the calibration calculations involving the minimization of the objective function. The Persistence reads the input information and output an update model including the new set of adjusted model parameters. The Facade takes all the user inputs through the GUI and performs validation and consistency-checking. In addition, the Facade provides the required interaction between the Domain and the Persistence. The tool was developed in Java; it includes 5801 lines of code. Figure number 1 represents the class diagram of the calibration software. Figure 2 represents a detailed class diagram

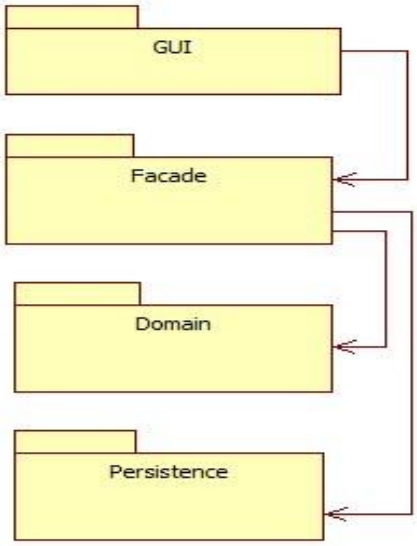

Figure 1.Class Diagram.

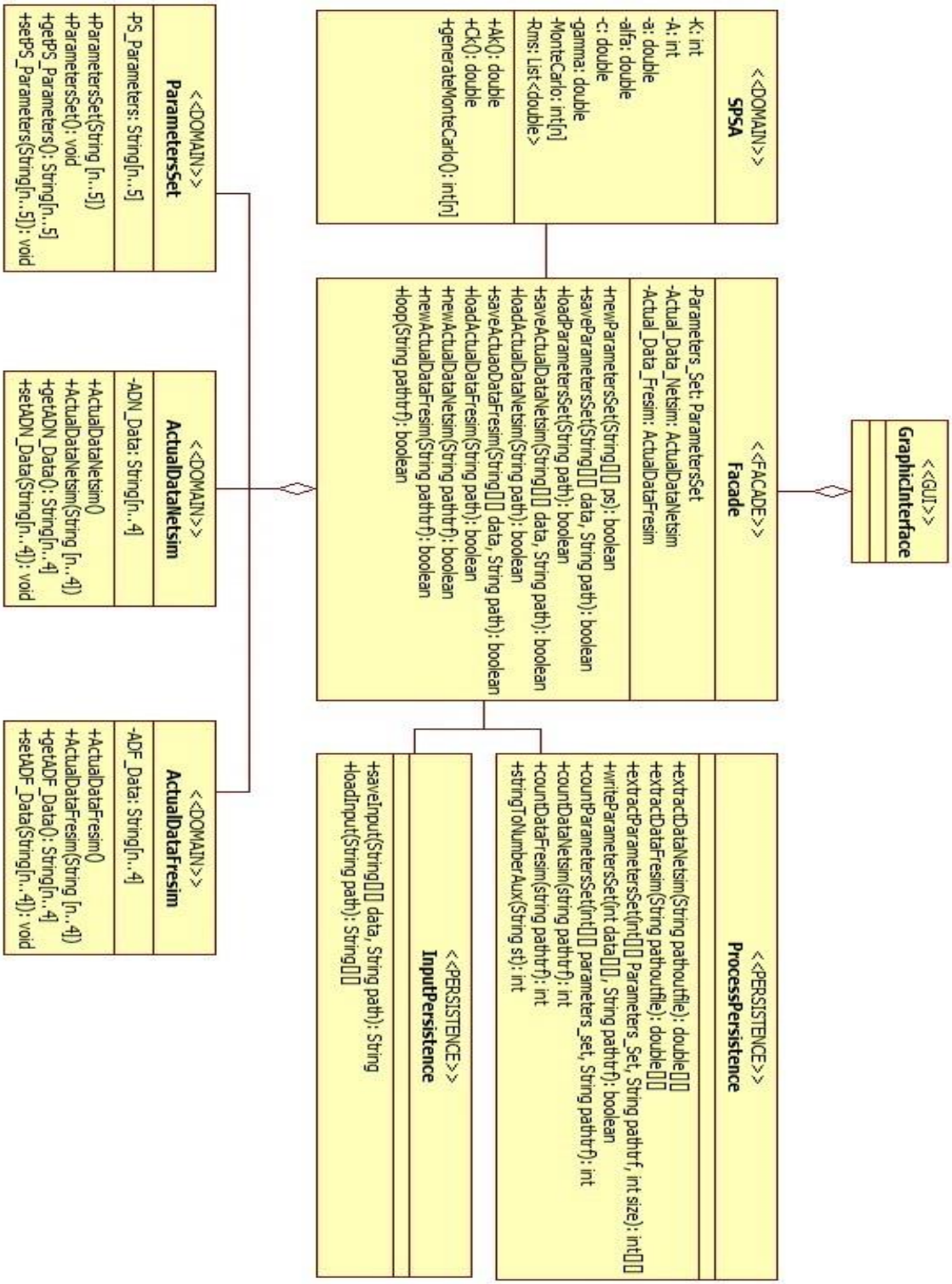

Figure 2. Detailed Class Diagram.

CHAPTER 4 EXPERIMENTS AND RESULTS

Micro-simulation Model

This study tested the proposed methodology using CORSIM models, which integrates two different models to represent a complete traffic system, FRESIM for freeways and NETSIM for surface streets (McTrans Center, 2010). *Traffic Analysis Toolbox Volume IV: Guidelines for Applying CORSIM Micro-simulation Modeling Software*(Holm et al., 2007) described a procedure for the calibration of micro-simulation traffic flow models, with a focus on CORSIM. The suggested procedure in these guidelines used three sequential and iterative steps, including the calibration of (i) capacity at key bottlenecks, (ii) traffic volumes, and (iii) system performance. However, the guidelines did not suggest any particular methodology to perform the calibration in an efficient and effective manner. For example, issues associated with convergence and stability of the solutions were not discussed. Nevertheless, alternative studies proposed and developed practical procedures to accelerate the calibration process, which typically is time consuming(Hourdakis, Michalopoulos, & Kottommannil, 2003). However, stability and convergence still are issues.

Results

Three experiments were designed to test the capabilities of the proposed methodology to calibrate based on vehicle counts and speeds simultaneously.

First Experiment: Pyramid Highway in Reno, NV

In this experiment a CORSIM model for a portion of the Pyramid Highway in Reno, NV, was calibrated. This portion of highway is located between Milepost 1.673 and 5.131.

This calibration focused on speeds and link counts for the entire simulation. The weight factor in the objective function was set to 0.7. The model included 126 arterial links, and no freeways were included. Link counts and speeds were only available for 45 of these links. Coefficients for the SPSA algorithm were selected using guidelines from the literature (Spall, 2003). These values affected the convergence of the algorithm.

Figure 3 *(a)* shows aGoogle map of the Pyramid Highway. Figure 3 *(b)* illustrates the corresponding CORSIM model.

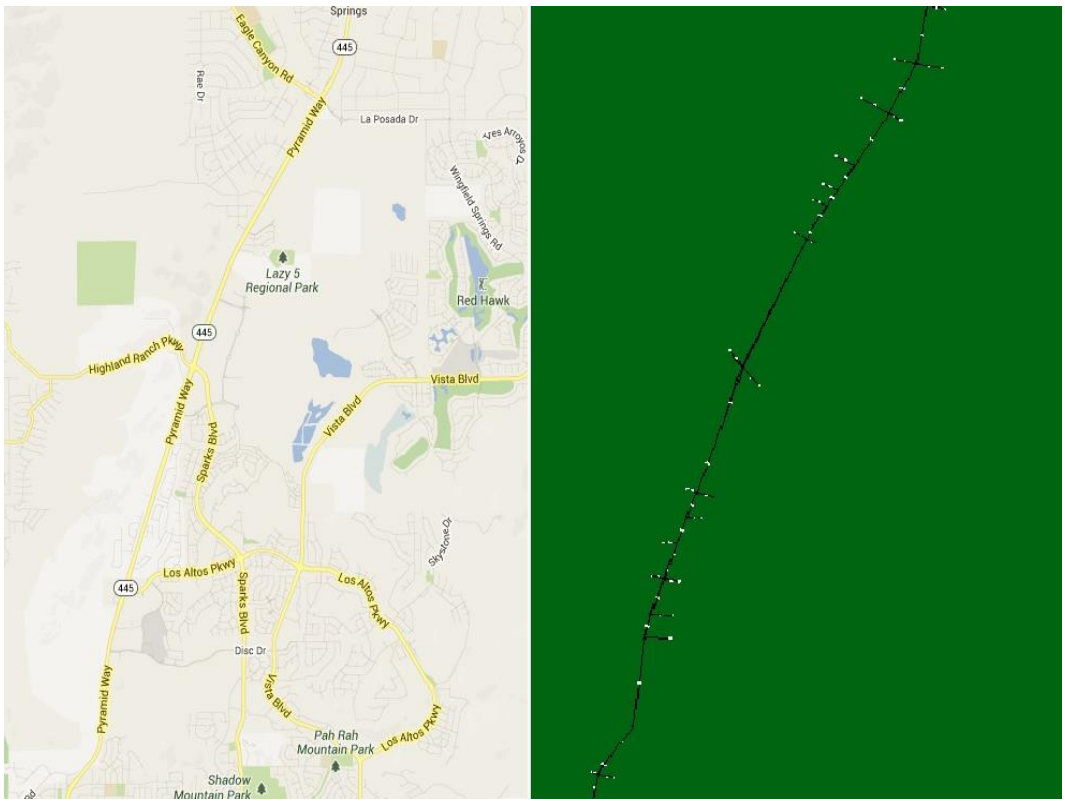

(a) ***(b)***

Figure 3. *(a)*Pyramid Highway, Reno, NV and *(b)*the CORSIM model for Pyramid Highway.

Figure 4 illustrates how the objective function was minimized. The noisy trajectory was a consequence of the stochastic perturbation applied to all calibration parameters to obtain

the gradient approximation at each iteration. The characteristics of the traffic model made the function noisier due to rounding. The *NRSM* was 0.042 before calibration and 0.010 after calibration. The calibration process stopped around the 80th iteration, when a stable region was found.

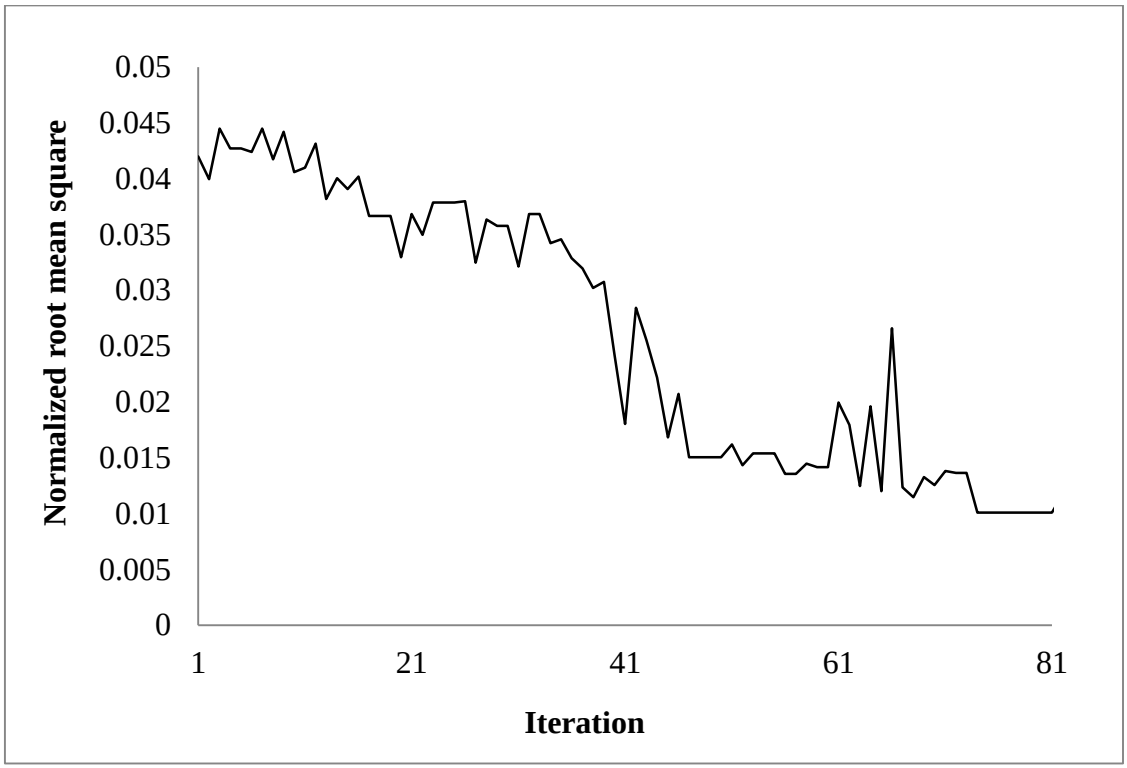

Figure 4. Objective function for the first experiment.

Figure 5 shows the actual and simulated counts before calibration. These values present poor initial conditions, especially for the volumes over 1500 vehicles per hour (vph). Figure 6 shows the actual and simulated counts after calibration. The proposed methodology is able to reduce the gap between actual and simulated counts. The results illustrate larger improvements for the large counts. Figure 6 clearly shows that links with counts over 1500 vph were improved, while the values with good initial conditions were slightly modified.

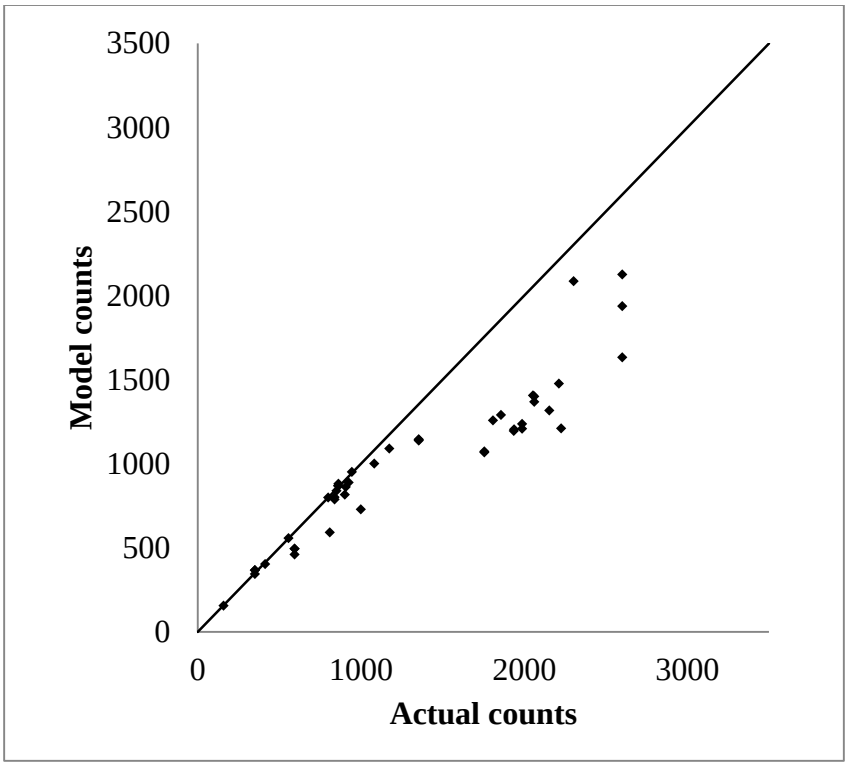

Figure 5. Actual vs. simulated counts before calibration.

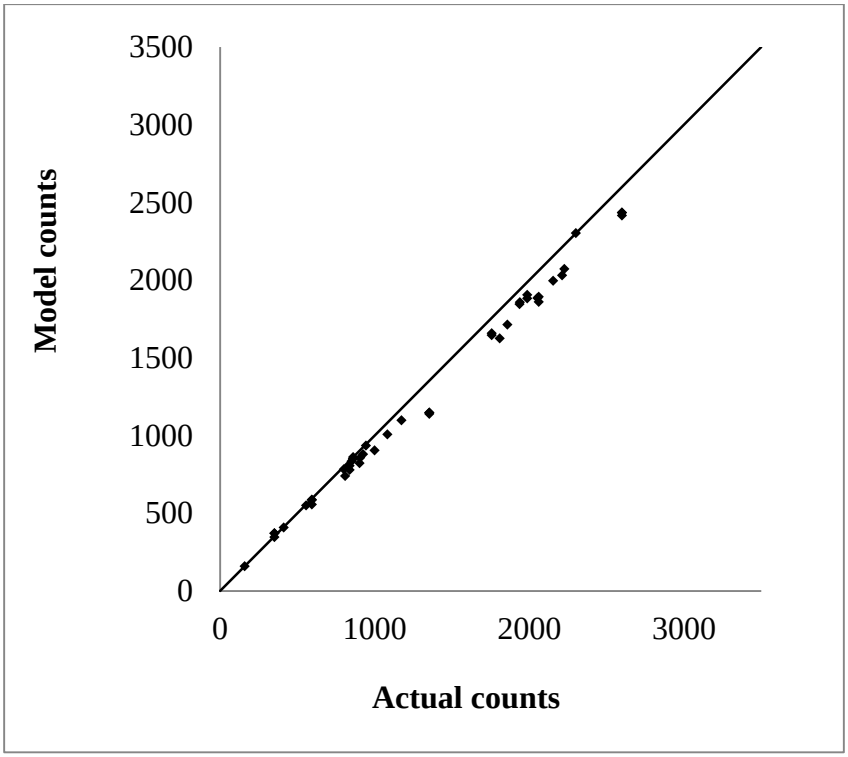

Figure 6. Actual vs. simulated counts after calibration.

Figure 7 shows actual and simulated speeds before calibration. As illustrated, simulated speeds are far from actual speeds. The simulation model underestimates many speed values.

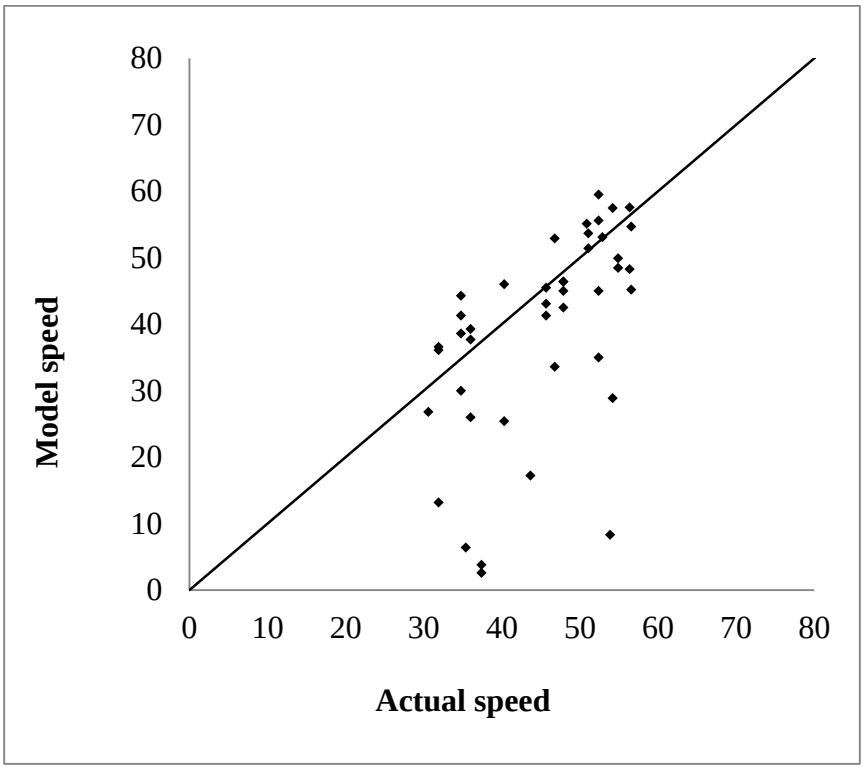

Figure 7. Actual vs. simulated speeds before calibration.

Figure 8 shows the speeds after calibration. In this case the speeds were improved for 23 of the links. The rest of the speeds were kept close to the initial values with a variation less than 1 mile per hour (mph). This can be associated to the relative large value of the weight assigned to the counts in the objective function ($W = 0.7$). In addition, the experimental results show that link counts are more sensitive than speeds to changes in the calibration parameters. Figure 8 shows the *GEH* statistics for the models before and after calibration. It is clear that the calibration model significantly improves the *GEH* statistic. All the links reach a *GEH* statistic less or equal to 5, thereby satisfying the calibration criteria. The results show that the three calibration criteria are satisfied. In

general, the proposed methodology was able to improve significantly the model outcomes.

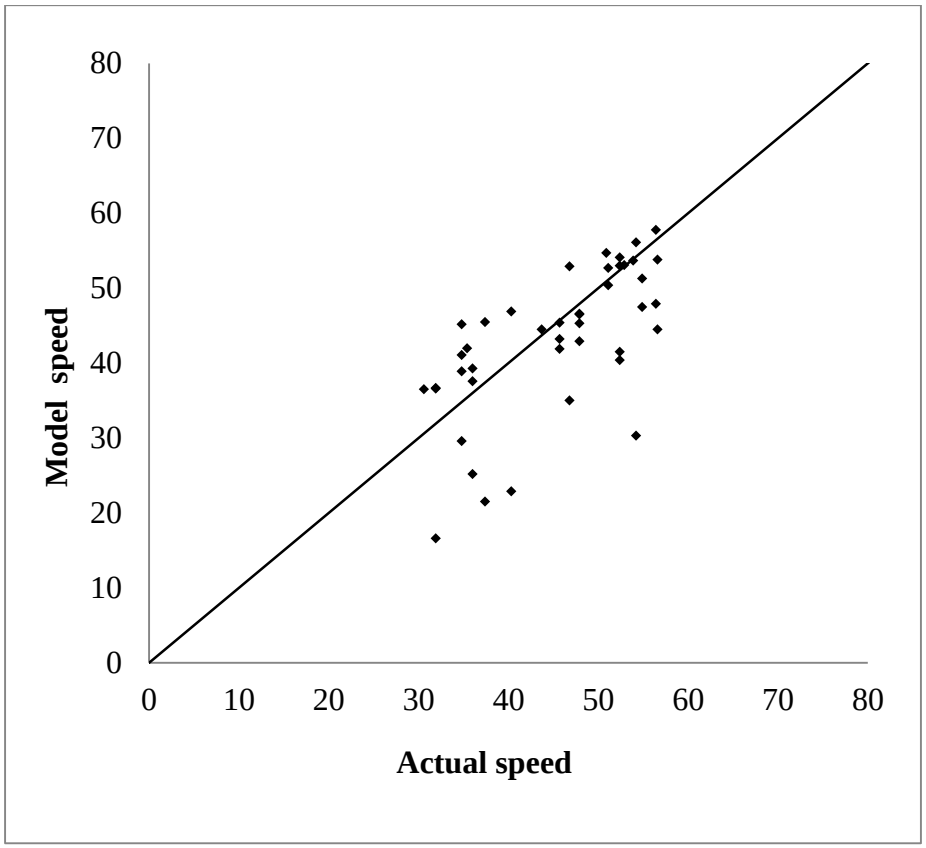

Figure 8. Actual vs. simulated speeds after calibration.

Table 2 summarizes the calibration results for the first experiment. The total difference between actual and simulated link counts is 6% for all links in the network, and the *GEH* statistic is less than 5 for all links; therefore, the calibration criteria is satisfied. Table 2 shows the *GEH* statistics for the model before and after calibration. It is clear that the calibration significantly improves the *GEH* statistic. The results show that the two calibration criteria are satisfied.

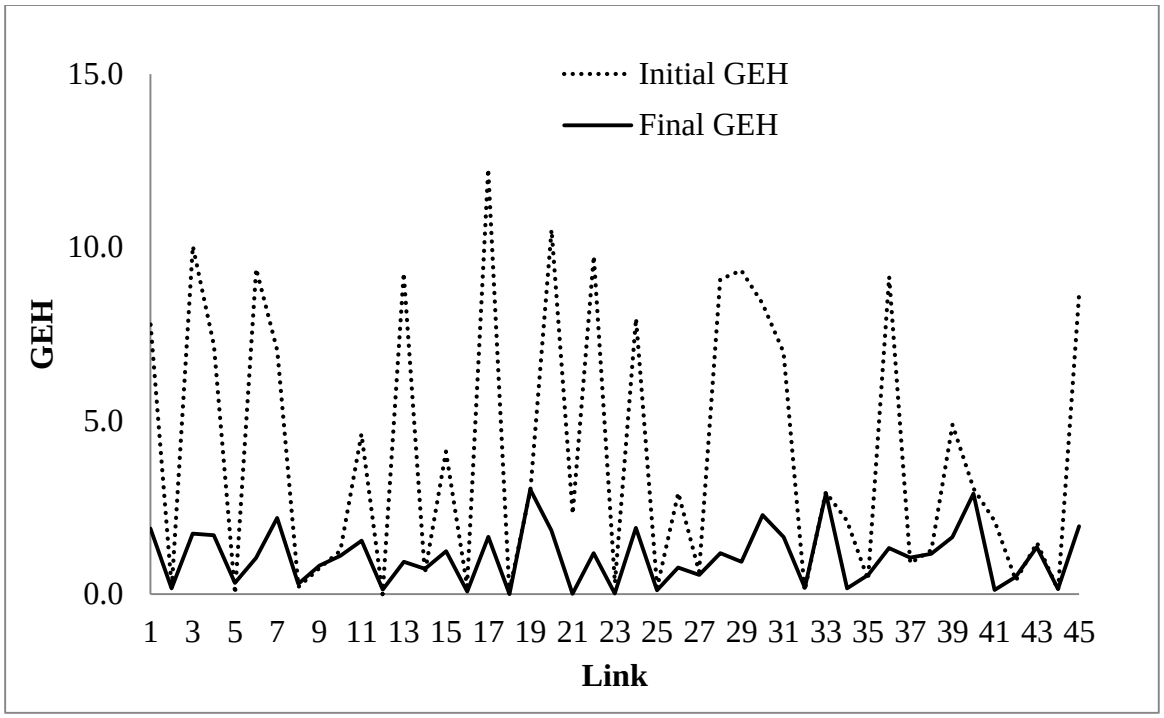

Figure 9. GEH Statistics for the first experiment.

Table 2. Summary of Calibration Results for the Second Experiment

	NRMS	Total link counts	GEH
Before calibration	0.042	45,359	< 5 for 74% of the cases
After calibration	0.010	55,882	< 5 for 100% of the cases
Actual		59,610	

Second Experiment: I-75 in Miami, FL

In this experiment, a portion of I-75 in Miami, FL was calibrated. A total of 375 freeway ramps and 334 arterial links were included in the model. Data was available for 353 freeway ramps and 59 arterial links for a morning peak period of one hour. The coefficients of the SPSA algorithm were the same as those used in the first experiment. All the calibration parameters in the network were included as well as the turning volumes for freeways and arterials.

Figure 10 *(a)* shows the Google map of I-75 highway in Miami, FL. Figure 10 *(b)* illustrates the corresponding CORSIM model.

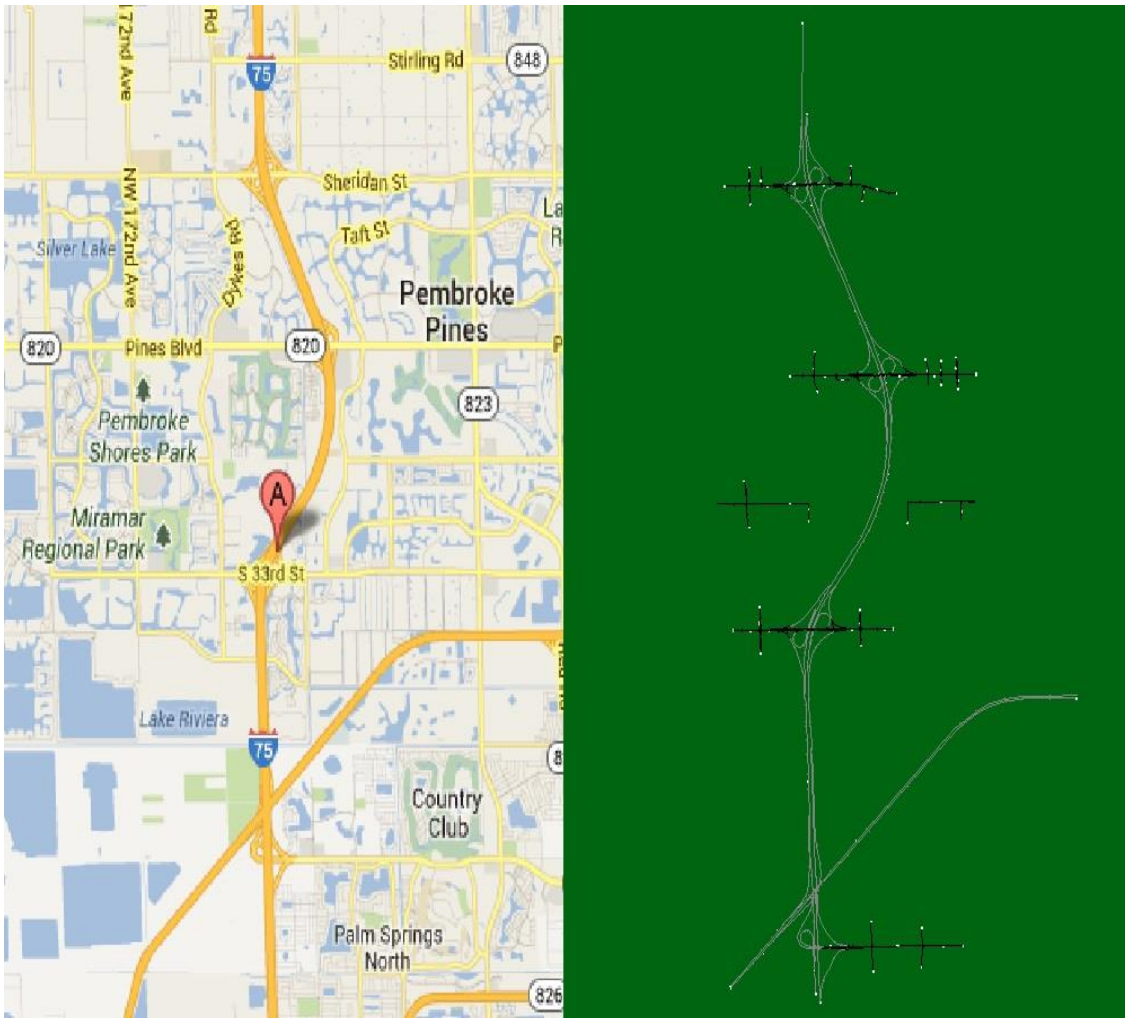

(a) ***(b)***

Figure 10. *(a)*I-75 in Miami, FL, and*(b)* the I-75 CORSIM model.

Figure 11 illustrates the trajectory of the objective function for this experiment. The *NRMS* goes from 0.270 to 0.245.

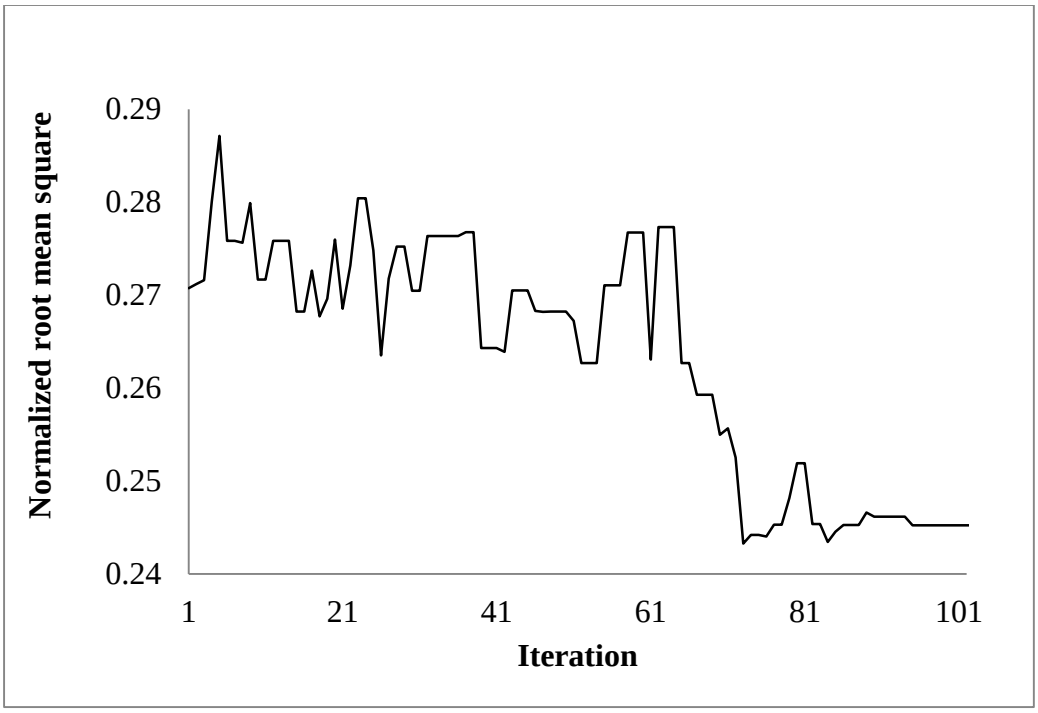

Figure 11. Objective function for the second experiment.

Figure 12 illustrates the link counts for the ramp segments in the model before calibration. Figure 13 shows the link counts for the ramps after calibration. These results clearly show that the calibration process significantly reduces the difference between actual and simulated link counts.

Figure 14 shows the *GEH* statistics for the ramps in the model before and after calibration. It is clear that the calibration model significantly improves the *GEH* statistic. 99.6% of the links reach a *GEH* statistic less or equal to 5, thereby satisfying the calibration criteria.

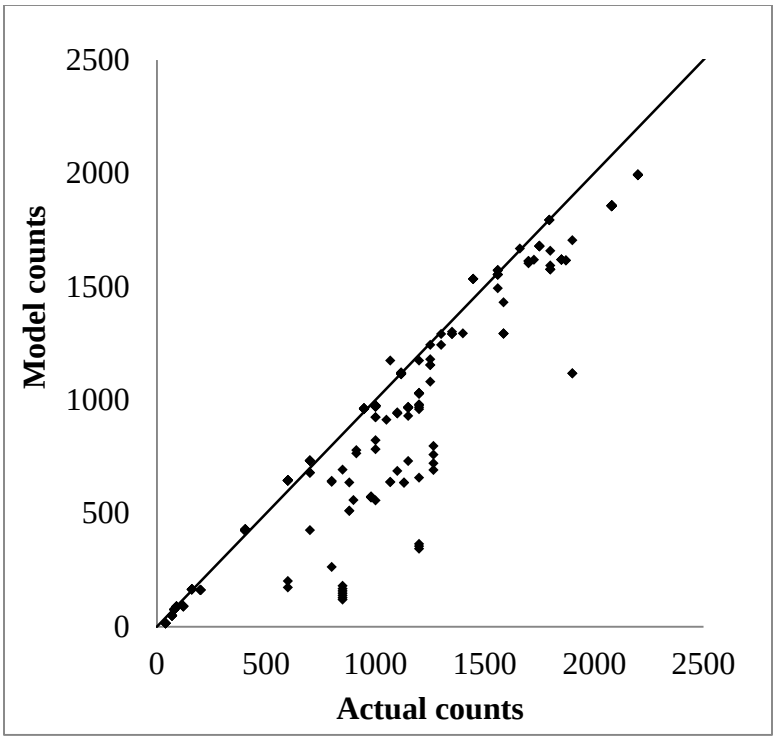

Figure 12. Links counts before calibration for freeway ramps in the network.

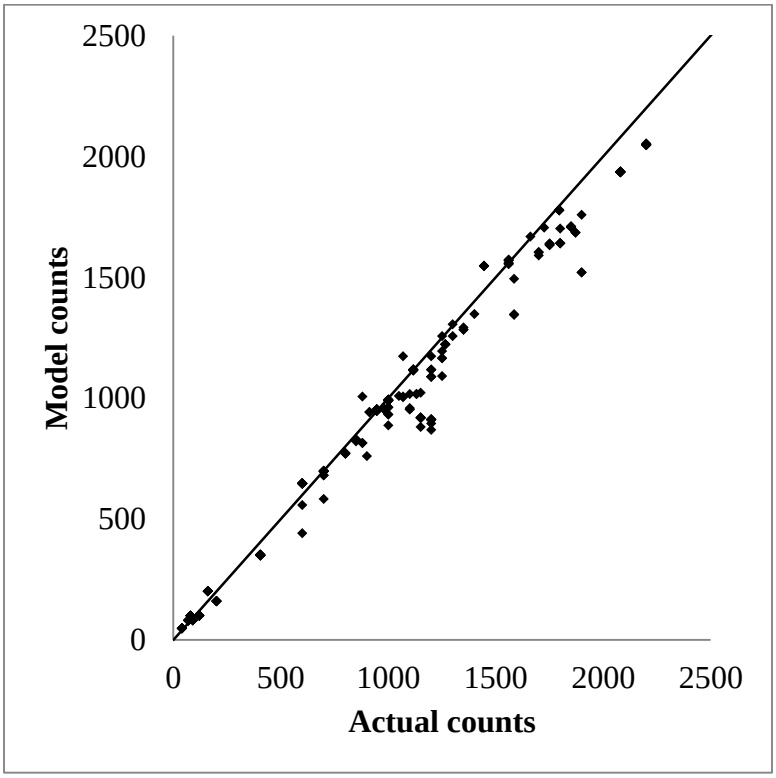

Figure 13. Links counts after calibration for freeway ramps in the network.

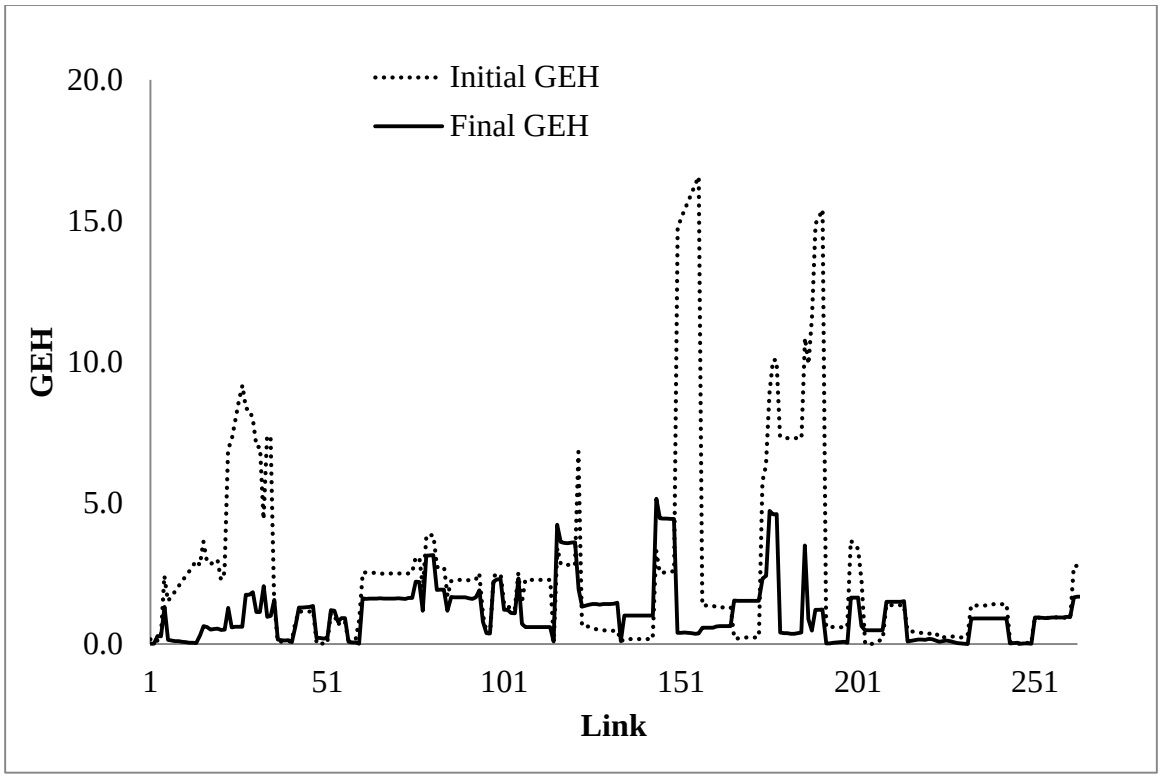

Figure 14. GEH Statistics for the arterial part of the second experiment.

Figure 15 illustrates the link counts for the arterials before calibration. Figure 16 shows the link counts for the ramps after calibration. These results show that there is significant improvement for links with large link counts.

Figure 17 shows the *GEH* statistics for the ramps in the model before and after calibration. The calibration model significantly improves the *GEH* statistic. Seventy-six percent (76%) of the links reach a *GEH* statistic less or equal to 5.

Figure 13 and Figure 16 together show that the calibration methodology provides better results for freeway ramps than for arterials. This could be a consequence of having more data available for freeway ramps than for arterials, thereby giving more weight to the ramps.

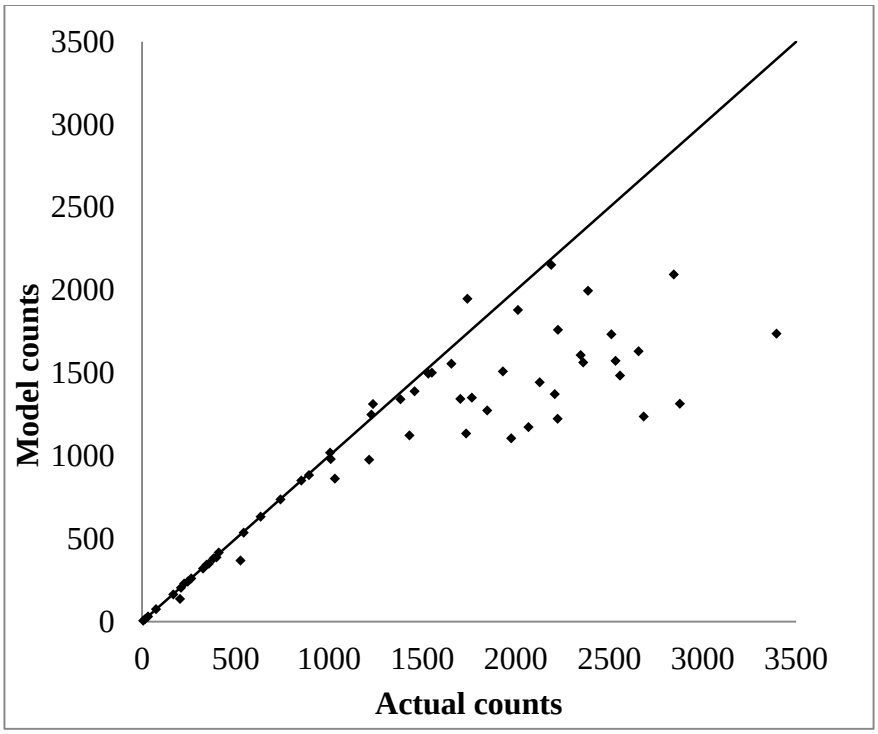

Figure 15. Links counts before calibration for the arterials in the network.

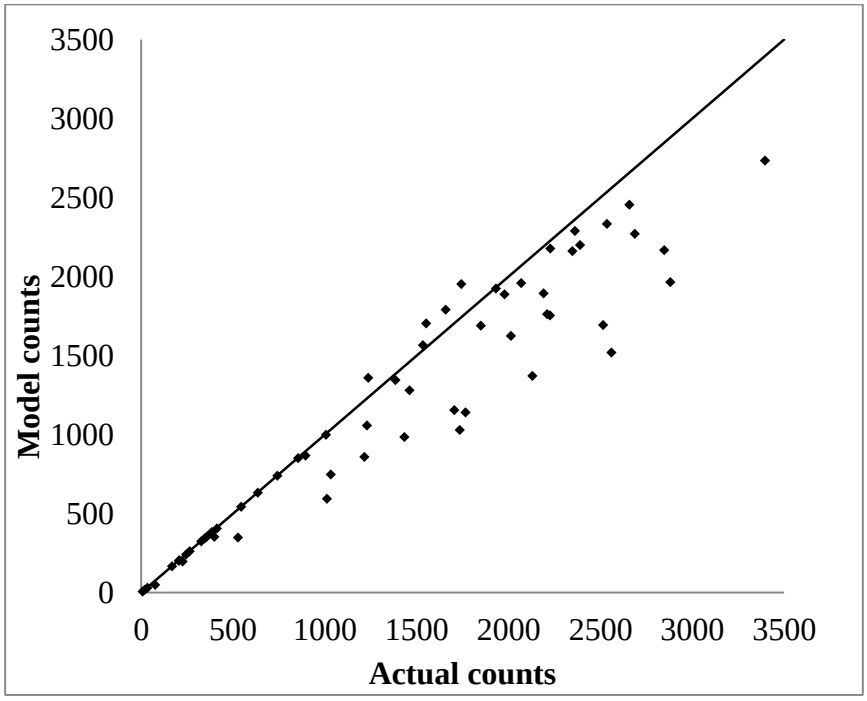

Figure 16. Links counts after calibration for the arterials in the network.

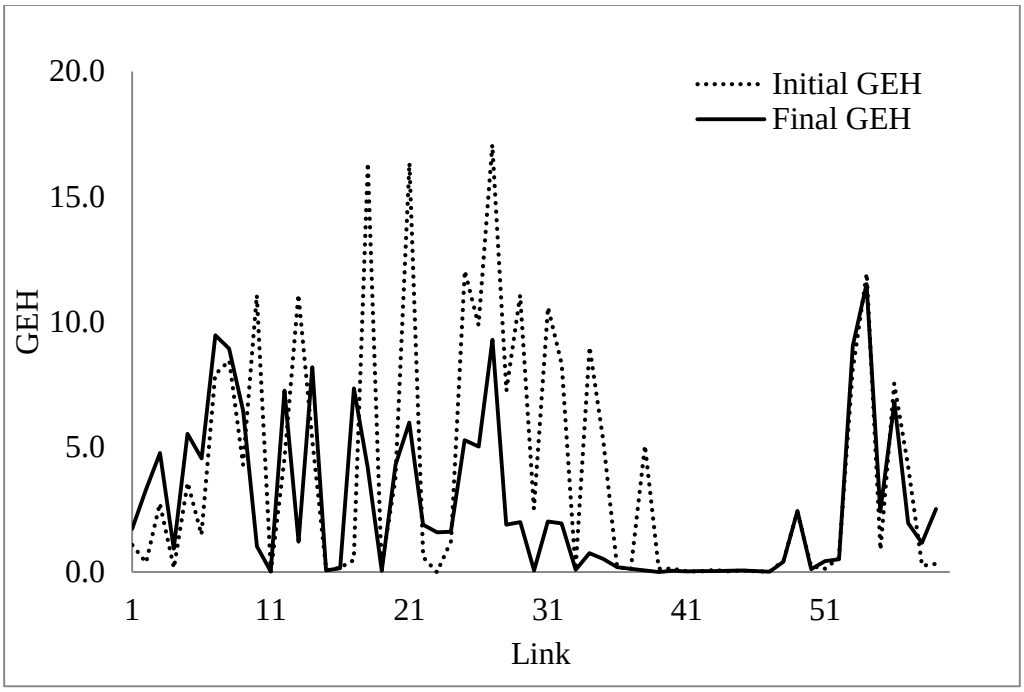

Figure 17. GEH Statistics for the freeway part of the second experiment.

Table 3 shows the 'before' and 'after' GEH statistics. As illustrated, the calibration improves the statistics, especially for the highest GEHs. However, some GEH values need to be improved because they are over 5.

Table 3. Summary of Calibration Results for the Second Experiment

		Total link counts (vph)	**GEH**
FREEWAY	Before calibration	234,928.2	< 5 for 86% of the cases
	After calibration	257,454.1	< 5 for 99.6% of the cases
	Actual	271,908	
ARTERIALS	Before calibration	61,097	< 5 for 66% of the cases
	After calibration	68,927	< 5 for 76% of the cases
	Actual	80,524	

Third Experiment: Network from McTrans Sample Data Sets

In this experiment, a network with arterials from McTrans official web page was calibrated. A total of 20 arterial links were included in the model. Data was available for all arterial links.

The total simulation time was 1hour divided in 4 time periods of 15 minutes each. In this experiment, all parameters for all links for all four time periods were updated. The coefficients of the SPSA algorithm were the same as those used in the previous experiments. All the calibration parameters in the network as well as the turning volumes were included.

Figure 18 shows the CORSIM model for this experiment.

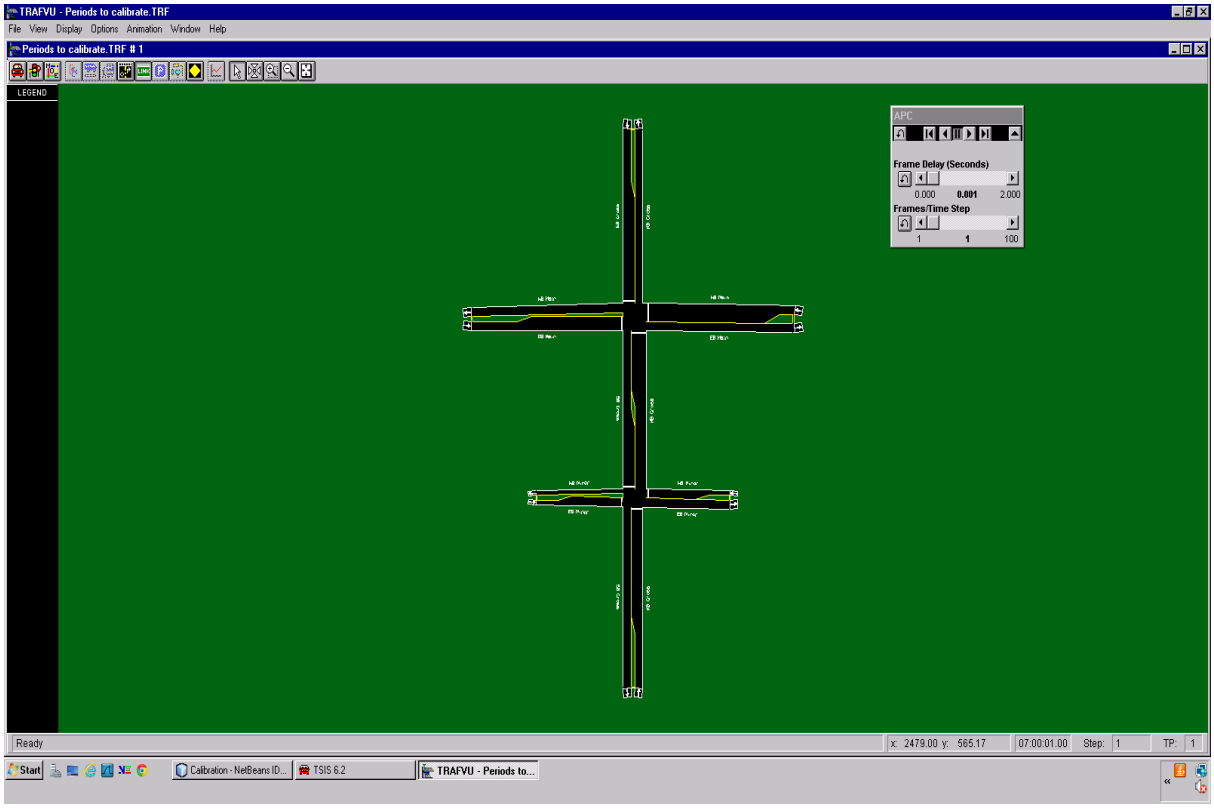

Figure 18. CORSIM Model for the third experiment.

Figure 19 illustrates the trajectory of the objective function corresponding to the third experiment. The initial NRMS value is 0.51, while the minimum obtained after 100 iterations of the optimization algorithm is 0.09.

Figure 19.Objective function for the third experiment.

Figure 20, Figure 21 and Figure 22, respectively, illustrate the link counts before and after the calibration, the speeds, and GEH statistics results for all links in the network for the first time period of the simulation. These results clearly show that the calibration process significantly reduces the difference between actual and simulated link counts.

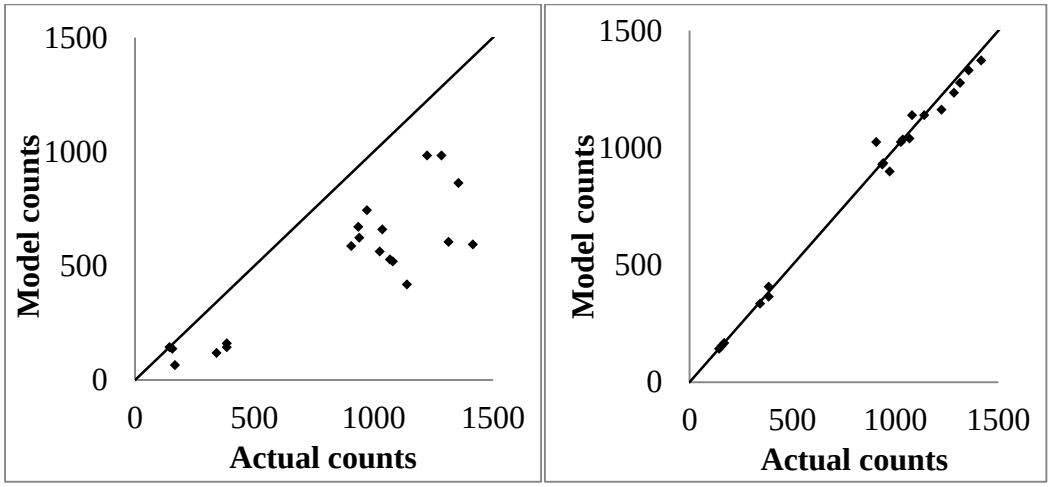

Figure 20. Actual vs. simulated counts *(a)*before and *(b)*after calibrationfor time period1.

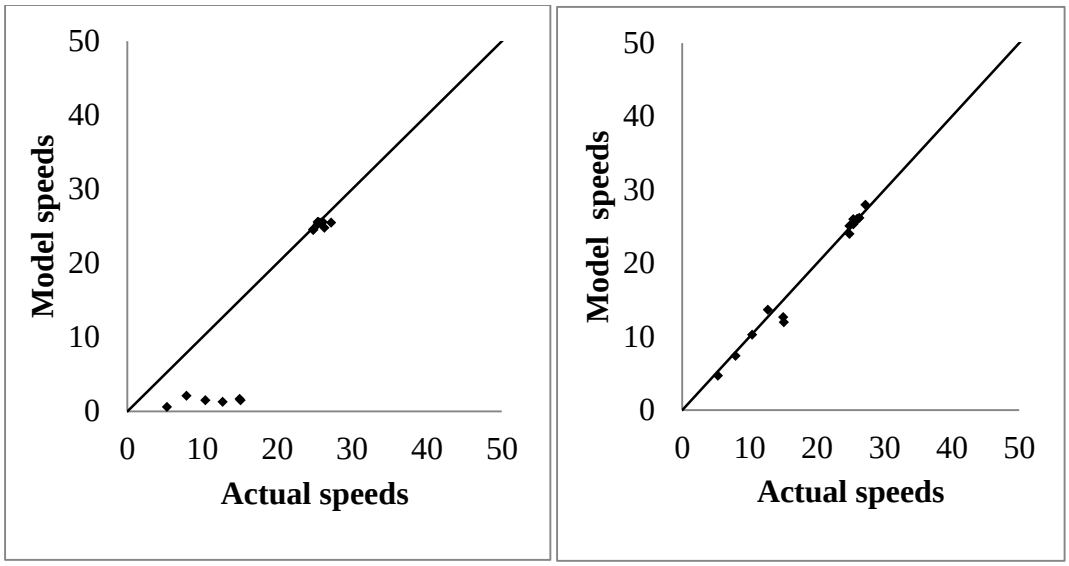

Figure 21. Actual vs. simulated speeds *(a)*before and *(b)*after calibration for time period 1.

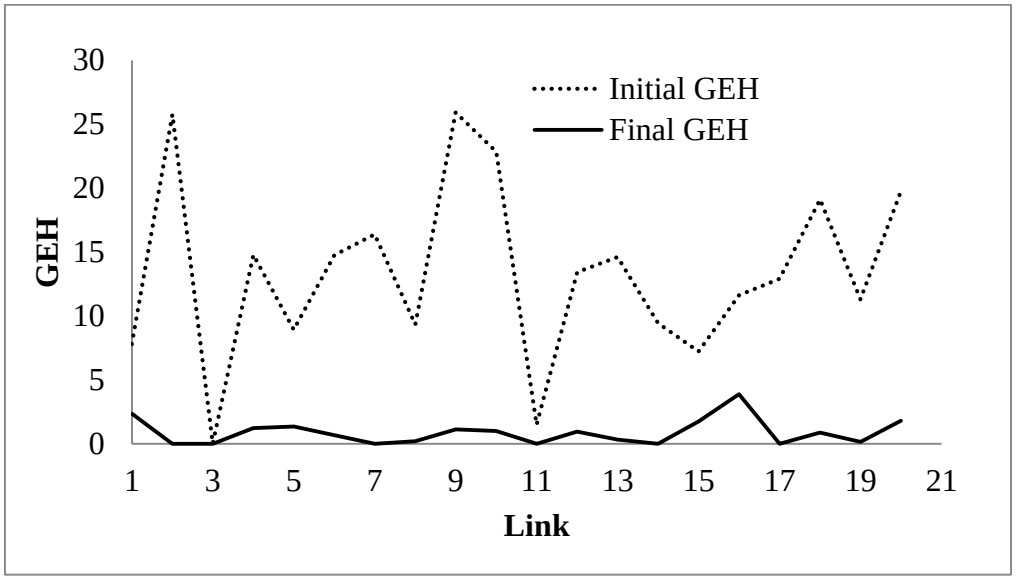

Figure 22. GEH Statistics for time period 1 of the third experiment.

Similar to Figure 20 to Figure 22, Figure 23 to Figure 32 show the link counts, speeds, and GEH statistics results for all links in the network for the second, third, and fourth time period, respectively, of the simulation. The calibrated results are significantly closer to the actual values, relative to the 'before calibration' results. In addition, all links have a GEH statistic below the threshold limit of 5.

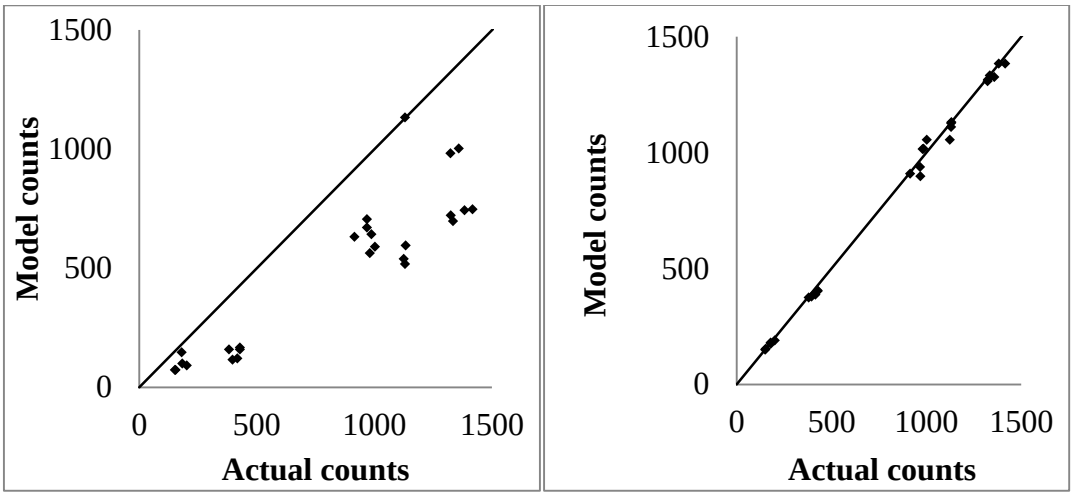

Figure 23. Actual vs. simulated counts (a) before and (b) after calibration for time period 2.

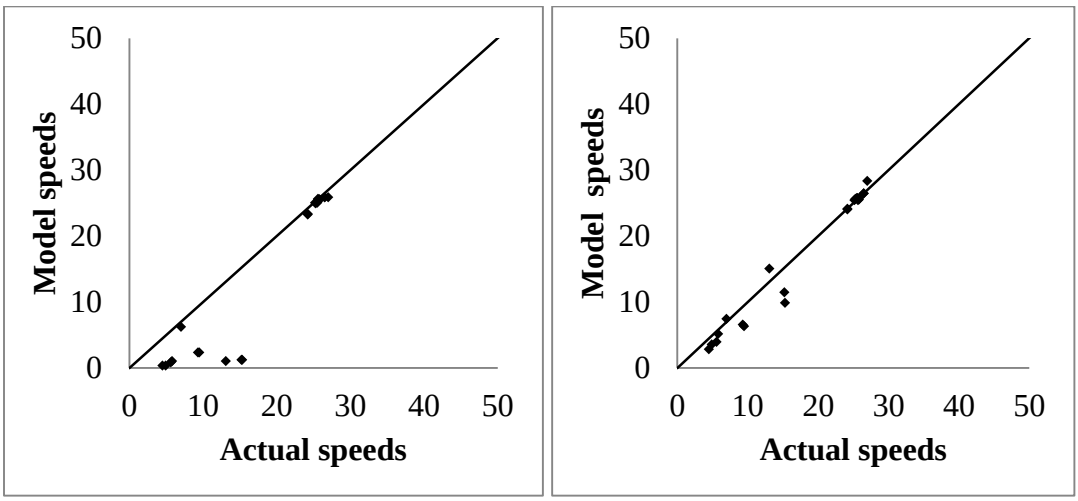

Figure 24. Actual vs. simulated speeds *(a)*before and *(b)*after calibration for time period 2.

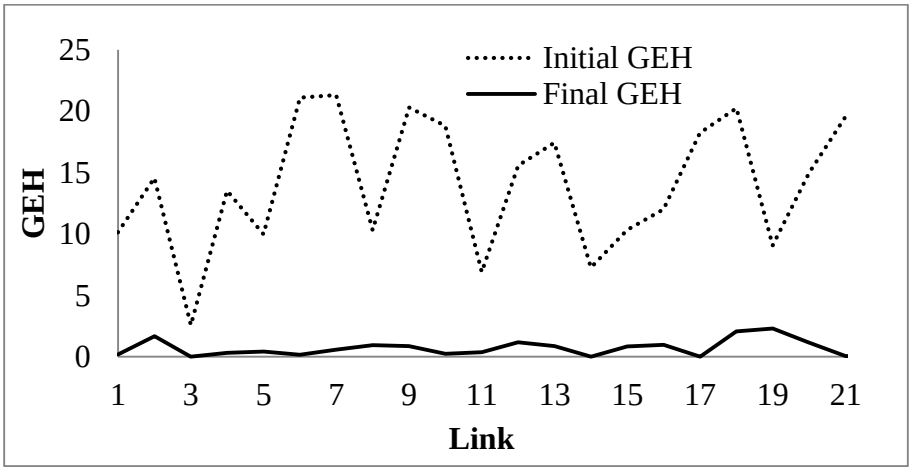

Figure 25. GEH Statistics for time period 2 of the third experiment.

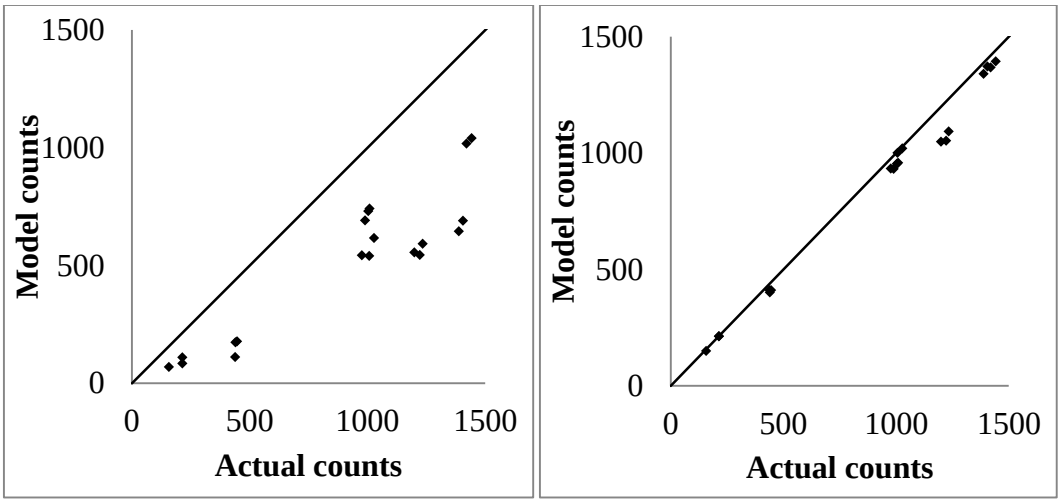

Figure 26. Actual vs. simulated counts before (a) and after (b) calibration for time period 3.

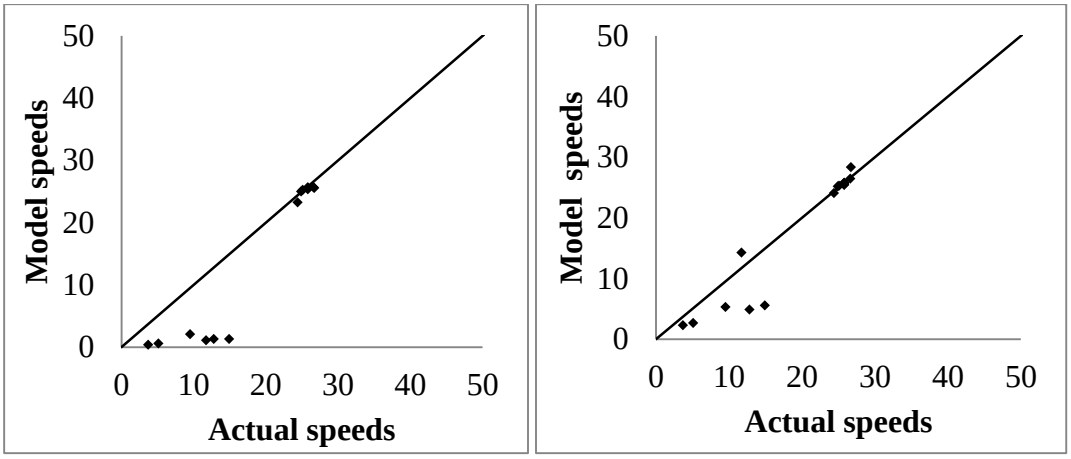

Figure 27. Actual vs. simulated speeds before (a) and after (b) calibration for time period 3.

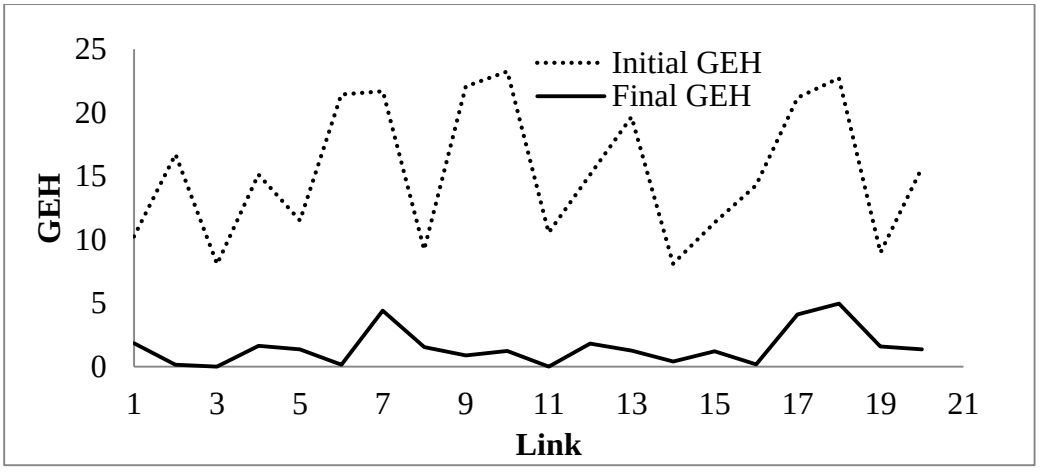

Figure 28. GEH Statistics for the third experiment time period 3.

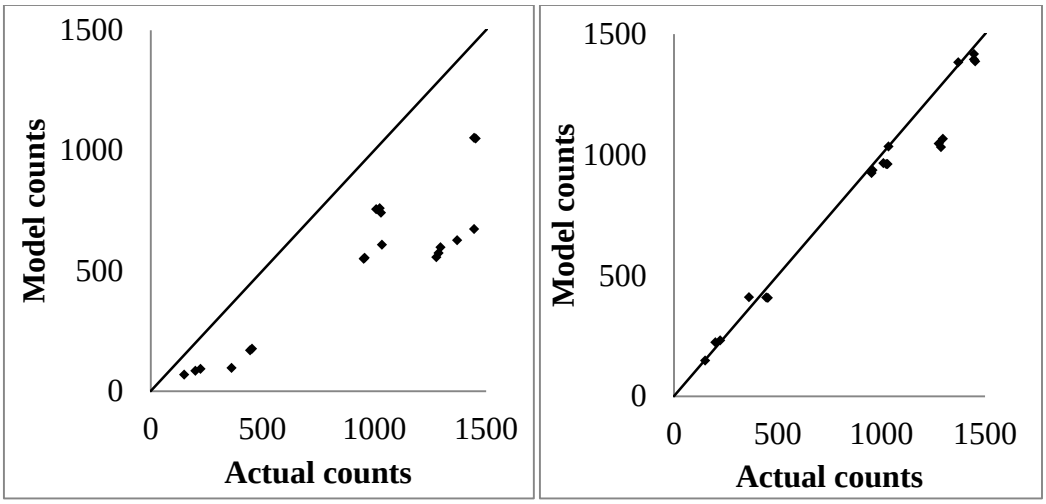

Figure 29. Actual vs. simulated counts before (a) and after (b) calibration for time period 4.

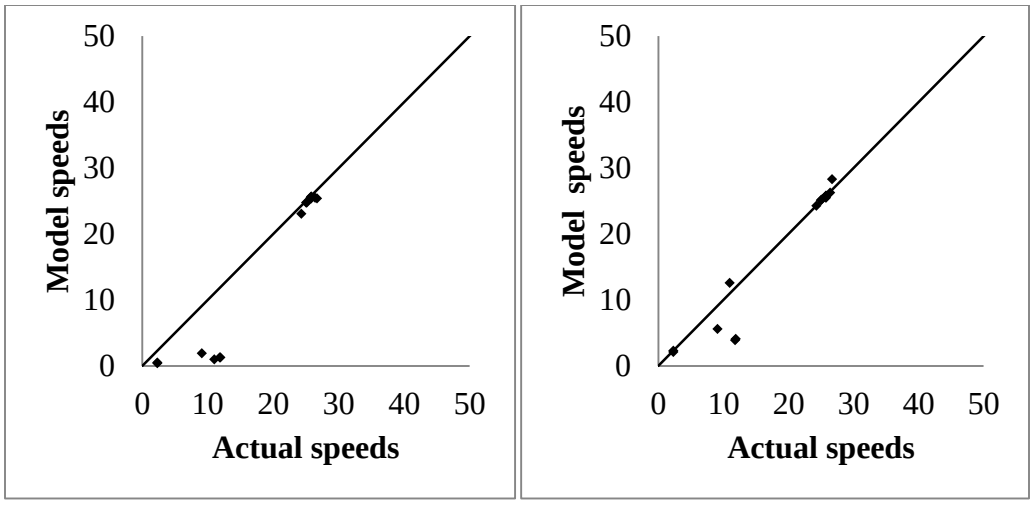

Figure 30. Actual vs. simulated speeds before *(a)* and after *(b)* calibration for time period 4.

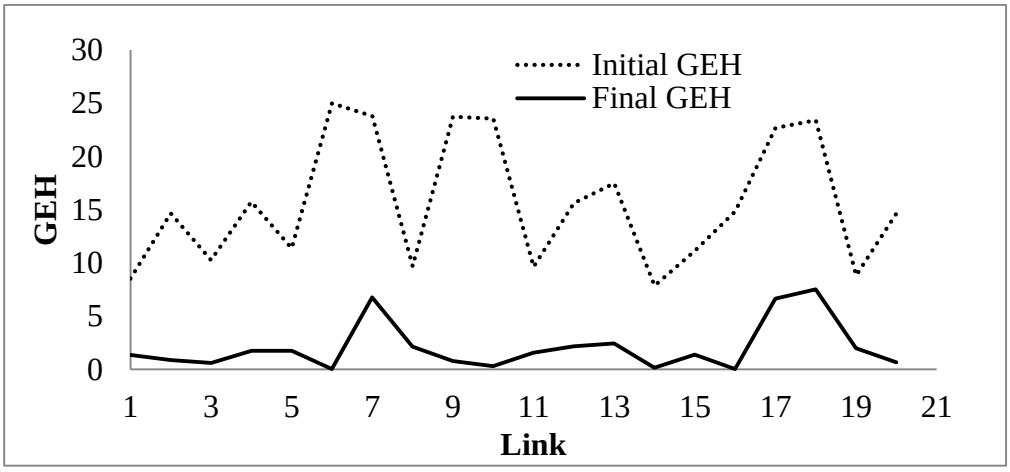

Figure 31. GEH Statistics for the third experiment time period 4.

In this experiment, optimal parameters for the model were determined in order to reproduce time-dependent link counts and speeds. The calibrated parameters took a single value during the entire simulation process; that is, they were not time-dependent. In contrast, the link counts were time-dependent. These results illustrate the ability of the proposed calibration methodology to adjust model parameters so as to calibrate the time-dependent link counts.

The summary of the results are showed in Table 4.

Table 4. Summary of the Calibration Results for the Third Experiment

		Total link counts (vph)	**GEH**
Time period 1	Before calibration	10,126	< 5 for 10% of the cases
	After calibration	17,136	< 5 for 100% of the cases
	Actual	17,276	
Time period 2	Before calibration	13,498	< 5 for 10% of the cases
	After calibration	22,625	< 5 for 100% of the cases
	Actual	22,891	
Time period 3	Before calibration	10,502	< 5 for 0% of the cases
	After calibration	17,820	< 5 for 100% of the cases
	Actual	18,767	
Time Period 4	Before calibration	10,533	< 5 for 0% of the cases
	After calibration	17,939	< 5 for 95% of the cases
	Actual	19,013	

Calibration and Validation

In order to validate calibration results, a new calibration was performed. The Reno Network from the first experiment was used for this validation. In the first experiment this network was calibrated using 45 link counts. The GEH statistics were lower than 5 for all the cases. In addition 23 link speeds were improved and the rest kept close to the initial values. In this validation the same network is calibrated using only 25 actual link counts and speeds. After the calibration, the GEH statistics were lower than 5 for 100% of the links, speeds showed similar results as the calibration of the first experiment with 26 link speeds improved. Figures 32 and 33 show the before and after vehicle counts and GEH statistics, respectively. These results imply that the proposed methodology has the capability provide adequate performance for an actual calibration effort.

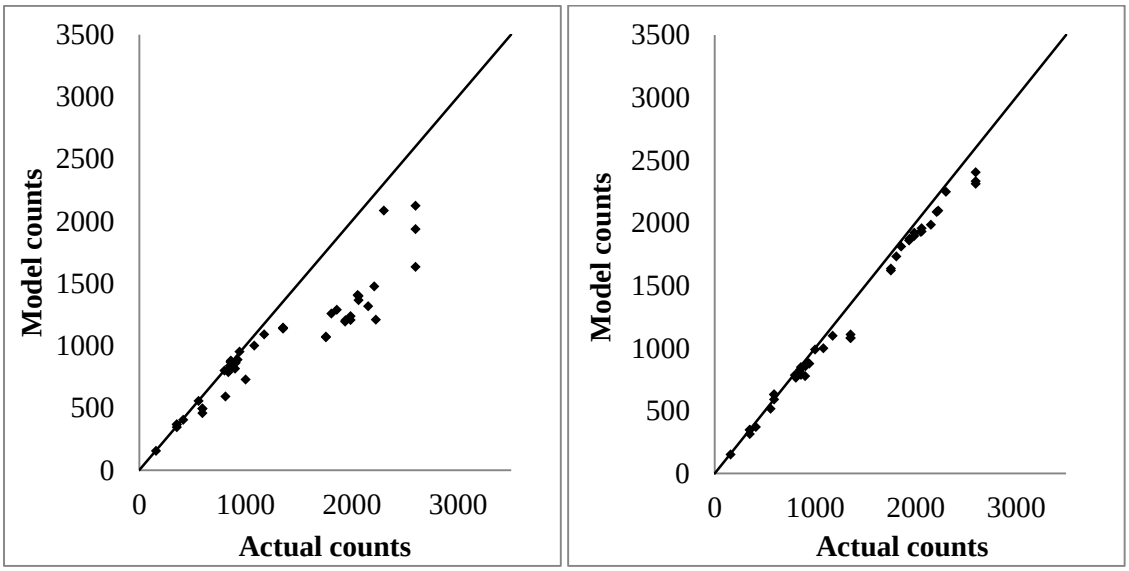

Figure 32. Actual vs. simulated counts before (a) and after (b) calibration.

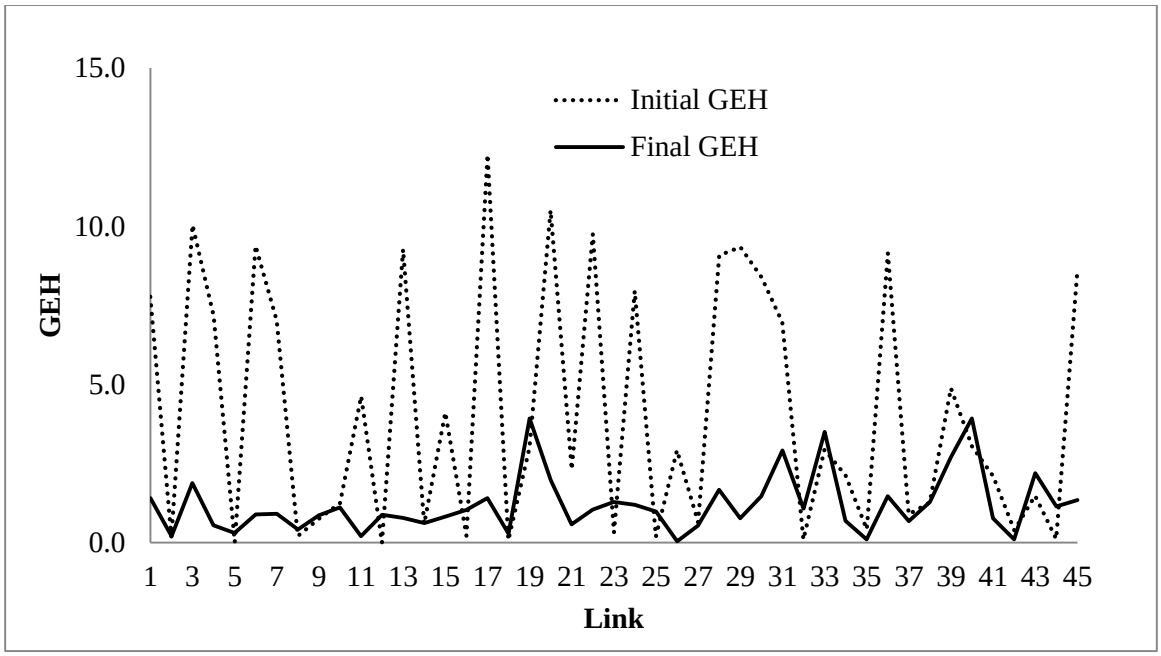

Figure 33. GEH Statistics for the validation

CHAPTER 5 CONCLUSIONS AND FUTURE WORK

Conclusions

This study proposes a methodology for the calibration of micro-simulation traffic flow models. The design and implementation of this methodology seeks to enable the calibration of generalized models. The proposed calibration methodology is being developed independent of characteristics for any particular microscopic traffic flow simulation model. At this point in the model development, the proposed methodology minimizes the difference between actual and simulated time dependent link counts and speeds by considering all model parameters and turning volumes simultaneously.

The methodology used the Simultaneous Perturbation Stochastic Approximation (SPSA) algorithm to determine the calibrated set of model parameters. Previous studies have proposed the use of the SPSA algorithm for the calibration of vehicular traffic systems. However, few parameters were considered, and the calibration typically was based on a single performance measure, usually link counts. The simultaneous consideration of all model parameters and multiple performance measures is motivated by issues associated with convergence and stability. During the experiments, the proposed algorithm always reached convergence and stability.

The same set of calibration parameters was used in all the experiments. Therefore, any effort during parameter selection has been eliminated. The results were improved for the entire model. All calibrated parameters were within reasonable boundaries. Similarly, no irregularities were observed using the graphical user interface.

The proposed methodology was tested using CORSIM models. However, there is nothing preventing the implementation of the proposed methodology for the calibration

of other models. Three different vehicular traffic systems were calibrated, taking into consideration all their model parameters by using various performance measures, including link counts and speeds. The first experiment included arterials, using as performance measures link counts and speeds. The second system included both arterials and freeways. Considering arterials and freeways represented a significant challenge because two different models with different parameters needed to be considered simultaneously. The third experiment included time-dependent link counts and speeds for four time periods during this experiment; in addition, global, individual, and time-dependent parameters were considered.

The experimental results illustrated the effectiveness of the proposed methodology. The three vehicular traffic systems used in this study were successfully calibrated; specifically, the calibration criteria were satisfied after the calibration was performed. The quality of the second vehicular traffic system improved significantly. However, further sensitivity analysis of the parameters used by the SPSA algorithm is required to achieve better results and satisfy the calibration criteria. Further, as the number of parameters required for calibration increases, the complexity of the optimization problem also increases as well as the complexity to determine the set of required optimization coefficients.

Future Work

The calibration tool developed as part of this study used an optimization algorithm that required a set of coefficients to find the appropriate set of CORSIM model parameters. A time-consuming sensitivity analysis of these coefficients was required to achieve desired results.

A bi-level optimization framework is required to enable the simultaneous calibration of traffic flow and SPSA parameters. The first level of the bi-level framework represents the existing calibration tool developed as part of the existing project, whose objective was the calibration of CORSIM models under saturated conditions. Here, and Simultaneous Perturbation Stochastic Approximation (SPSA) optimization algorithm was used to determine the appropriate calibration parameters. The second level of the proposed bi-level framework corresponds to future research, whose objective is to automate the sensitivity analysis that is required to find the right set of optimization coefficients for the SPSA algorithm.

Figure 34 illustrates a potential implementation of the proposed bi-level framework for the simultaneous calibration and sensitivity analysis. The white boxes represent the existing calibration tool developed under the existing project. The gray boxes represent the proposed approach for the sensitivity analysis that will be developed as part of the new research project. A pseudo-fuzzy control process is proposed to find the right set of coefficients that will enable the desired calibration. The fuzzy control process has the capability to capture the learning process that a user has obtained after calibrating many networks using the calibration tool. That is, the knowledge from the calibration tools

development can be transferred to the fuzzy control process in order to enable the determination of the right set of optimization coefficients.

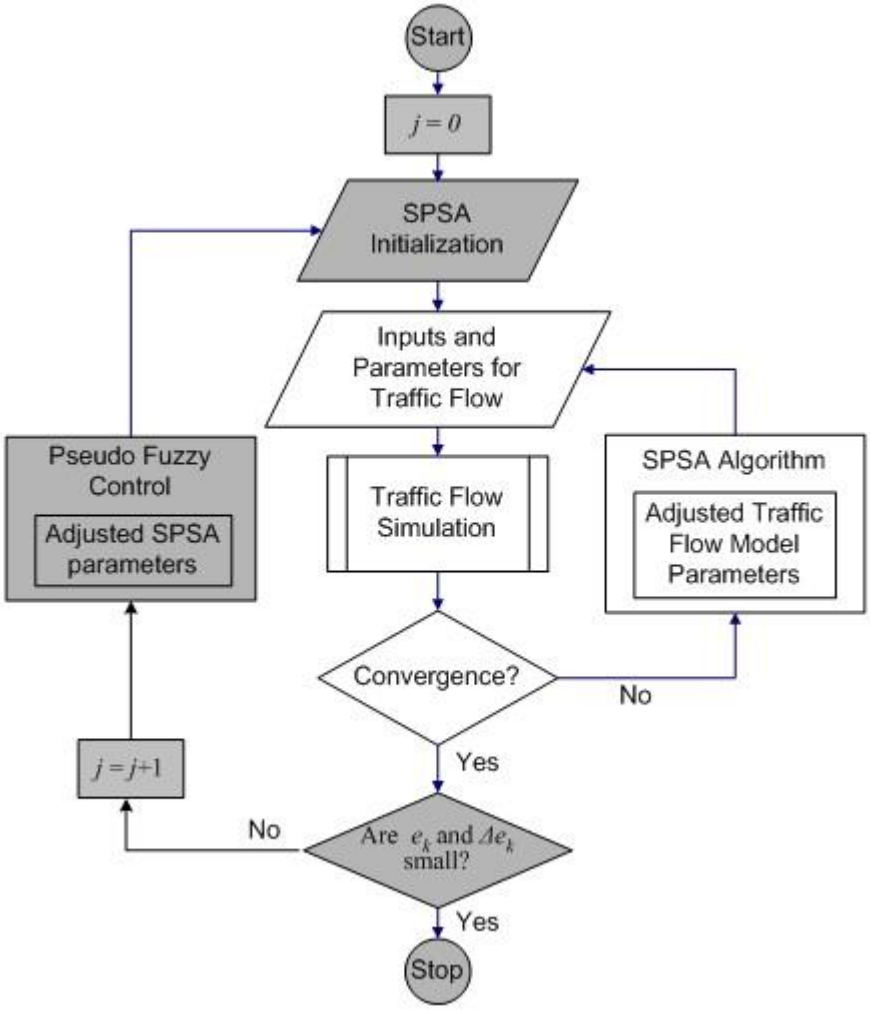

Figure 34. Bi-level optimization framework for calibration and sensitivity analysis.

APPENDIX A CALIBRATION PARAMETERS

Calibration Parameters for CORSIM Models

The calibration of CORSIM models can involve Driver Behavior and Vehicle Performance parameters (McTrans Center, 2010).These parameters can be defined exclusively for surface streets or freeways or both models simultaneously. In addition, the resolution of these parameters can be global or link-based defined. This study considered all types of parameters and levels of resolution. In addition, parameters related to demand patterns were included. Tables A4 and A5 show the different parameters used for the calibration of CORSIM models. Several studies have included sensitivity analysis of the calibration parameters for CORSIM models. These studies have showed that maximum the parameters associated with 'non emergency deceleration rates', for example, do not affect the outcomes of a specific FRESIM model. However, the specific vehicle distributions improve the accuracy of that model (Schultz &Rilett, 2004). Driver behavior parameters were found to affect the time to breakdown and the ramps flow. In contrast, flow parameters showed to produce low effects (Kondyli et al., 2012). The calibration parameters have different effects for specific networks and conditions. The interaction between these parameters is very complex and might vary from model to model. Our methodology decreases the effort during the selection of the calibration parameters by creating a default set of parameters and modifying their defaults ranges in order to avoid unrealistic values. Tables A7 to A9 show examples of the parameters and the ranges used for the experiments conducted in this project. Due the large number of parameters, these tables include only a sub set of the total parameters calibrated during the experiments.

Table A5. Calibration Parameters for NETSIM Models

NETSIM Model – Surface streets		
Driver Behavior	**Vehicle Performance**	**Demand Patterns**
• Queue discharge headway • Start-up lost time • Distribution of free-flow speed by driver type • Mean duration of parking maneuvers • Lane change parameters • Maximum left and right turning speeds • Probability of joining spillback • Probability of left turn jumpers and laggers • Gap acceptance at stop signs • Gap acceptance for left and right turns • Pedestrian delays • Driver familiarity with their path	• Speed and acceleration characteristics • Fleet distribution and passenger occupancy	• Surface street turn movements

Table A6. Calibration Parameters for FRESIM Models

FRESIM Model - Freeways		
Driver Behavior	**Vehicle Performance**	**Demand Patterns**
• Mean start-up delay at ramp meters • Distribution of free flow speed by driver type • Incident rubbernecking factor • Car-following sensitivity factor • Lane change gap acceptance parameters • Parameters that affect the number of discretionary lane changes	• Speed and acceleration characteristics • Fleet distribution and passenger occupancy • Maximum deceleration values	• Freeway turn movements

Table A7. Examples of Calibration Parameters for the First Experiment

Number	Model	Parameter	Units	Link	Lower bound	Upper bound	Value before calibration	Value after calibration
1	NETSIM	Mean value of start-up lost time	Tenths of seconds	1-26	10	60	40	18
2	NETSIM	Mean value of start-up lost time	Tenths of seconds	1-41	10	60	42	12
3	NETSIM	Mean value of start-up lost time	Tenths of seconds	2-38	10	60	40	14
4	NETSIM	Mean value of start-up lost time	Tenths of seconds	3-27	10	60	42	38
5	NETSIM	Mean value of start-up lost time	Tenths of seconds	4-33	10	60	42	32
6	NETSIM	Mean queue discharge headway	Tenths of seconds	4-35	14	60	38	56
7	NETSIM	Mean queue discharge headway	Tenths of seconds	5-42	14	60	36	30
8	NETSIM	Mean queue discharge headway	Tenths of seconds	6-48	14	60	40	46
9	NETSIM	Mean queue discharge headway	Tenths of seconds	7-18	14	60	38	33
10	NETSIM	Mean queue discharge headway	Tenths of seconds	7-19	14	60	36	42
11	NETSIM	Percentage of drivers that know only one turn movement	Percentage		0	100	5	3
12	NETSIM	Percentage of drivers that know two turn movement	Percentage		0	100	95	97
13	NETSIM	Free-Flow speed adjustment for driver type 1	Percentage		0	1000	75	65
14	NETSIM	Free-Flow speed adjustment for driver type 2	Percentage		0	1000	85	75
15	NETSIM	Free-Flow speed adjustment for driver type 3	Percentage		0	1000	91	103
16	NETSIM	Left-Turning traffic	Percentage	10-11	0	9999	92	183
17	NETSIM	Trough traffic	Percentage	10-11	1	9999	1648	1878
18	NETSIM	Right turning traffic	Percentage	10-11	0	9999	0	0
19	NETSIM	Diagonal-Turning traffic	Percentage	10-11	0	9999	0	0
20	NETSIM	Left-Turning traffic	Percentage	11-10	0	9999	0	0
21	NETSIM	Trough traffic	Percentage	11-10	1	9999	636	836
22	NETSIM	Right turning traffic	Percentage	11-10	0	9999	37	7

23	NETSIM	Diagonal-Turning traffic	Percentage	11-10	0	9999	0	0
24	NETSIM	Left-Turning traffic	Percentage	2-3	0	9999	0	0
25	NETSIM	Trough traffic	Percentage	2-3	1	9999	2156	2009
26	NETSIM	Right turning traffic	Percentage	2-3	0	9999	104	93
27	NETSIM	Diagonal-Turning traffic	Percentage	2-3	0	9999	0	0
28	NETSIM	Duration of a lane-change maneuver	Seconds		2	5	2	5
29	NETSIM	Mean time for a driver to react to sudden deceleration of the lead vehicle	Tenths of seconds		5	15	5	8
30	NETSIM	Acceptable gap for driver type 1	Tenths of seconds		45	67	45	63
31	NETSIM	Acceptable gap for driver type 2	Tenths of seconds		40	60	40	58
32	NETSIM	Acceptable gap for driver type 2	Tenths of seconds		37	55	37	52

Table A8. Examples of Calibration Parameters for the Second Experiment

Number	Model	Parameter	Units	Link	Lower bound	Upper bound	Value before calibration	Value after calibration
1	FRESIM	Total number of vehicles with a thought movement	Percentage	416-9	0	9999	70	81
2	FRESIM	Total number of vehicles exiting at the off-ramp	Percentage	416-9	0	9999	30	19
3	FRESIM	Total number of vehicles with a thought movement	Percentage	14-15	0	9999	70	84
4	FRESIM	Total number of vehicles exiting at the off-ramp	Percentage	14-15	0	9999	30	16
5	FRESIM	Total number of vehicles with a thought movement	Percentage	28-29	0	9999	70	91
6	FRESIM	Total number of vehicles exiting at the off-ramp	Percentage	28-29	0	9999	30	9
7	FRESIM	Time to complete a lane changing maneuver	Tenths of seconds		10	40	20	22
8	FRESIM	Minimum separation of generation vehicles	Tenths of seconds		10	20	16	13
9	FRESIM	Car-following factor for vehicle type 1	Hundreds of seconds		100	150	125	104
10	FRESIM	Car-following factor for vehicle type 2	Hundreds of seconds		92	138	115	121
11	FRESIM	Car-following factor for vehicle type 3	Hundreds of seconds		84	126	105	122
12	FRESIM	Minimum acceleration lane speed to trigger upstream anticipatory lane changes	Miles per hour	5-6	37	47	43	44
13	FRESIM	Minimum acceleration lane speed to trigger upstream anticipatory lane changes	Miles per hour	17-18	37	47	43	46
14	FRESIM	Minimum acceleration lane speed to trigger upstream anticipatory lane changes	Miles per hour	35-36	37	47	43	44
15	FRESIM	Minimum acceleration lane speed to trigger upstream anticipatory lane changes	Miles per hour	60-61	37	47	43	44
16	FRESIM	Minimum acceleration lane speed to trigger upstream anticipatory lane changes	Miles per hour	72-74	37	47	43	44

17	NETSIM	Mean value of start-up lost time	Tenths of seconds	349-350	10	60	30	35
18	NETSIM	Mean value of start-up lost time	Tenths of seconds	350-349	10	60	30	14
19	NETSIM	Mean value of start-up lost time	Tenths of seconds	350-351	10	60	30	39
20	NETSIM	Mean queue discharge headway	Tenths of seconds	349-350	14	60	38	49
21	NETSIM	Mean queue discharge headway	Tenths of seconds	350-349	14	60	38	49
22	NETSIM	Mean queue discharge headway	Tenths of seconds	350-351	14	60	38	31
23	NETSIM	Left-Turning traffic	Percentage	350-351	0	9999	25	49
24	NETSIM	Trough traffic	Percentage	350-351	1	9999	40	49
25	NETSIM	Right turning traffic	Percentage	350-351	0	9999	35	37
26	NETSIM	Diagonal-Turning traffic	Percentage	350-351	0	9999	0	0
27	NETSIM	Left-Turning traffic	Percentage	352-351	0	9999	33	28
28	NETSIM	Trough traffic	Percentage	352-351	1	9999	43	35
29	NETSIM	Right turning traffic	Percentage	352-351	0	9999	23	37
30	NETSIM	Diagonal-Turning traffic	Percentage	352-351	0	9999	0	0
31	NETSIM	Duration of a lane-change maneuver	Seconds		2	5	3	5
32	NETSIM	Mean time for a driver to react to sudden deceleration of the lead vehicle	Tenths of seconds		5	15	10	5

Table A9. Examples of Calibration Parameters for the Third Experiment

Number	Model	Parameter	Units	Link	Time period	Lower bound	Upper bound	Value before calibration	Value after calibration
1	NETSIM	Mean value of start-up lost time	Tenths of seconds	11-21	1	10	60	50	43
2	NETSIM	Mean value of start-up lost time	Tenths of seconds	21-31	1	10	60	10	57
3	NETSIM	Mean value of start-up lost time	Tenths of seconds	41-31	1	10	60	50	15
4	NETSIM	Mean queue discharge headway	Tenths of seconds	11-21	1	14	60	18	43
5	NETSIM	Mean queue discharge headway	Tenths of seconds	21-31	1	14	60	90	22
6	NETSIM	Mean queue discharge headway	Tenths of seconds	41-31	1	14	60	18	20
7	NETSIM	Mean value of start-up lost time	Tenths of seconds	11-21	2	10	60	50	52
8	NETSIM	Mean value of start-up lost time	Tenths of seconds	21-31	2	10	60	10	59
9	NETSIM	Mean value of start-up lost time	Tenths of seconds	41-31	2	10	60	50	20
10	NETSIM	Mean queue discharge headway	Tenths of seconds	11-21	2	14	60	18	48
11	NETSIM	Mean queue discharge headway	Tenths of seconds	21-31	2	14	60	90	31
12	NETSIM	Mean queue discharge headway	Tenths of seconds	41-31	2	14	60	18	23
13	NETSIM	Mean value of start-up lost time	Tenths of seconds	11-21	3	10	60	50	45
14	NETSIM	Mean value of start-up lost time	Tenths of seconds	21-31	3	10	60	10	63
15	NETSIM	Mean value of start-up lost time	Tenths of seconds	41-31	3	10	60	50	16
16	NETSIM	Mean queue discharge headway	Tenths of seconds	11-21	3	14	60	18	47

17	NETSIM	Mean queue discharge headway	Tenths of seconds	21-31	3	14	60	90	17
18	NETSIM	Mean queue discharge headway	Tenths of seconds	41-31	3	14	60	18	18
19	NETSIM	Mean value of start-up lost time	Tenths of seconds	11-21	4	10	60	50	47
20	NETSIM	Mean value of start-up lost time	Tenths of seconds	21-31	4	10	60	10	51
21	NETSIM	Mean value of start-up lost time	Tenths of seconds	41-31	4	10	60	50	19
22	NETSIM	Mean queue discharge headway	Tenths of seconds	11-21	4	14	60	18	48
23	NETSIM	Mean queue discharge headway	Tenths of seconds	21-31	4	14	60	90	23
24	NETSIM	Mean queue discharge headway	Tenths of seconds	41-31	4	14	60	18	19
25	NETSIM	Percentage of drivers that know only one turn movement	Percentage		1	0	100	10	4
26	NETSIM	Percentage of drivers that know two turn movement	Percentage		1	0	100	90	96
27	NETSIM	Free-Flow speed adjustment for driver type 1	Percentage		1	0	1000	75	63
28	NETSIM	Free-Flow speed adjustment for driver type 2	Percentage		1	0	1000	85	81
29	NETSIM	Free-Flow speed adjustment for driver type 3	Percentage		1	0	1000	91	97
30	NETSIM	Left-Turning traffic	Percentage	11-21	1	0	9999	19	28
31	NETSIM	Trough traffic	Percentage	11-21	1	1	9999	857	875
32	NETSIM	Right turning traffic	Percentage	11-21	1	0	9999	166	154
33	NETSIM	Diagonal-Turning traffic	Percentage	11-21	1	0	9999	0	0
34	NETSIM	Left-Turning traffic	Percentage	21-31	1	0	9999	48	39
35	NETSIM	Trough traffic	Percentage	21-31	1	1	9999	425	418
36	NETSIM	Right turning traffic	Percentage	21-31	1	0	9999	625	635

37	NETSIM	Diagonal-Turning traffic	Percentage	21-31	1	0	9999	0	0
38	NETSIM	Left-Turning traffic	Percentage	41-31	1	0	9999	179	154
39	NETSIM	Trough traffic	Percentage	41-31	1	1	9999	550	523
40	NETSIM	Right turning traffic	Percentage	41-31	1	0	9999	424	397
41	NETSIM	Diagonal-Turning traffic	Percentage	41-31	1	0	9999	0	0
42	NETSIM	Duration of a lane-change maneuver	Seconds		1	2	5	2	4
43	NETSIM	Mean time for a driver to react to sudden deceleration of the lead vehicle	Tenths of seconds		1	5	15	10	8
44	NETSIM	Acceptable gap for driver type 1	Tenths of seconds		1	45	67	56	58
45	NETSIM	Acceptable gap for driver type 2	Tenths of seconds		1	40	60	50	60
46	NETSIM	Acceptable gap for driver type 2	Tenths of seconds		1	37	55	46	48

APPENDIX B CALIBRATION TOOL USER'S GUIDE

CORSIM categorizes all inputs into sets named, record types. Geometry, traffic flow, and calibration parameters are grouped in different record types. Inputs are stored in text files with extension .trf. A calibration tool was developed to implement the proposed calibration methodology to update all parameters in the .trf file. A graphical user interface (GUI) is used to facilitate the calibration process, which involves five steps as depicted below.

Step 1: Network Selection

The first step requires locating the .trf file with the corresponding CORSIM model. From the main menu, click on 'Select a .trf File' and browse to the location of the file in the disk.

Step 1: Calibration Tool -Main Menu

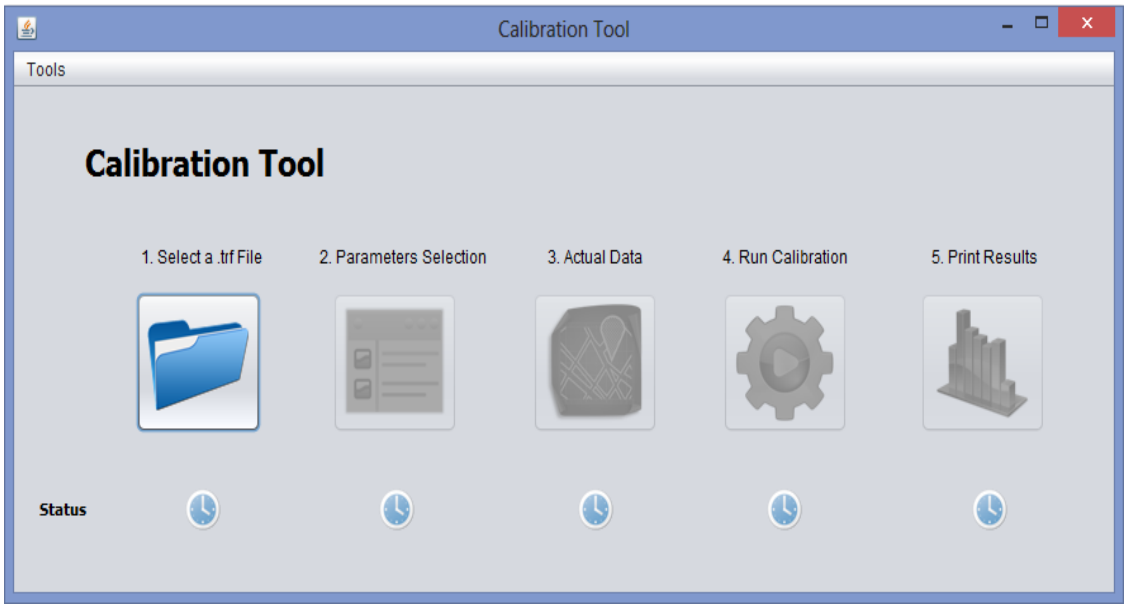

Browser

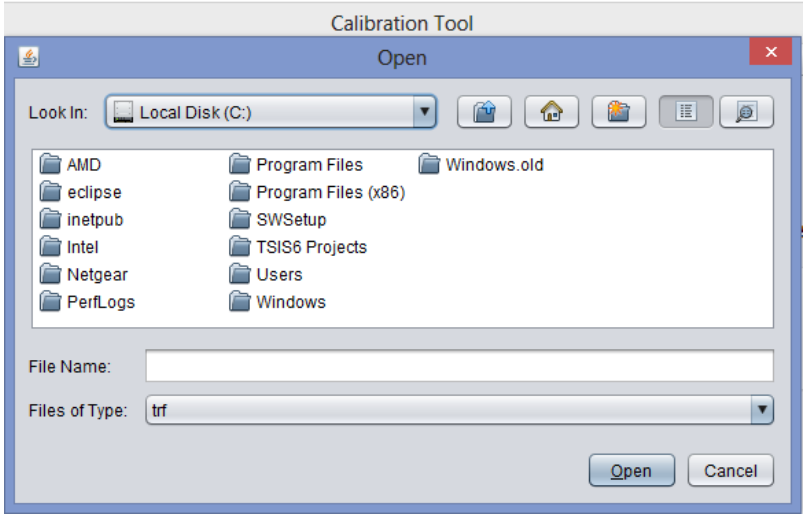

Step 2: Parameter Selection

In this step, the parameters for calibration are selected along with their initial values. Default values are available through 'Use Default Parameters'. However, these parameters can be edited as desired or required by using the editor menu, as shown below.

Parameter Selection

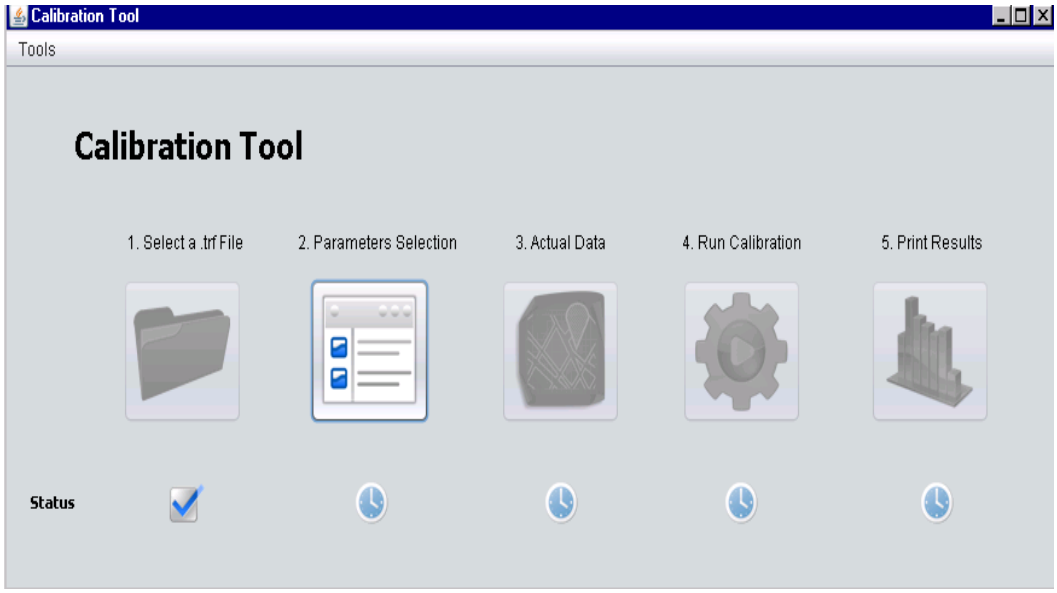

Parameters Editor

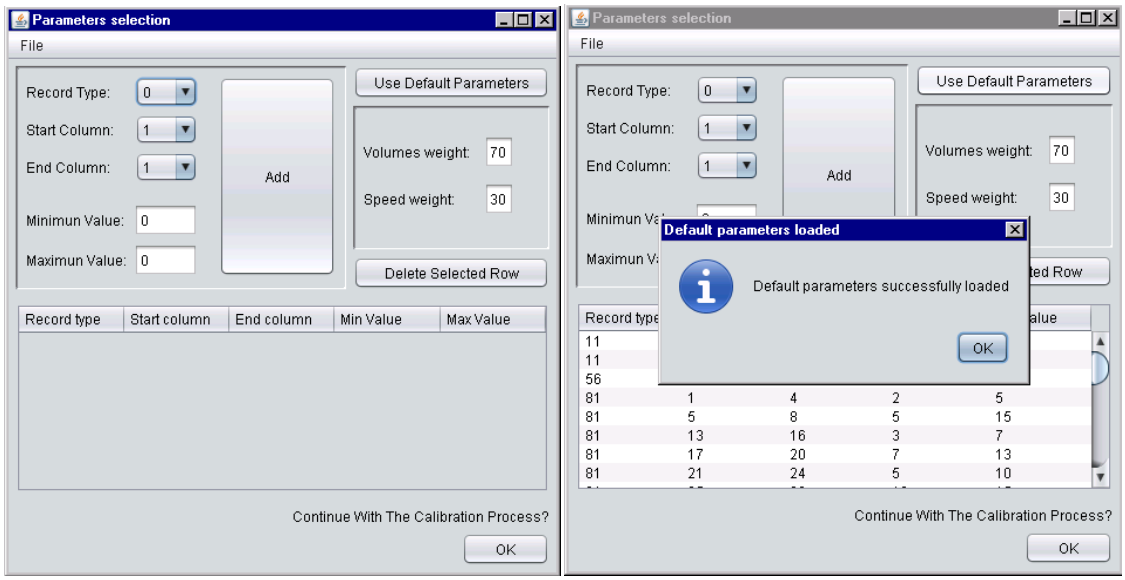

Step 3: Loading of Actual Data

This step involves loading the actual vehicle counts and/or speeds for calibration. An editable table is provided for the user to enter manually the available data. This table allows saving and modifying values at any time.

Actual Data

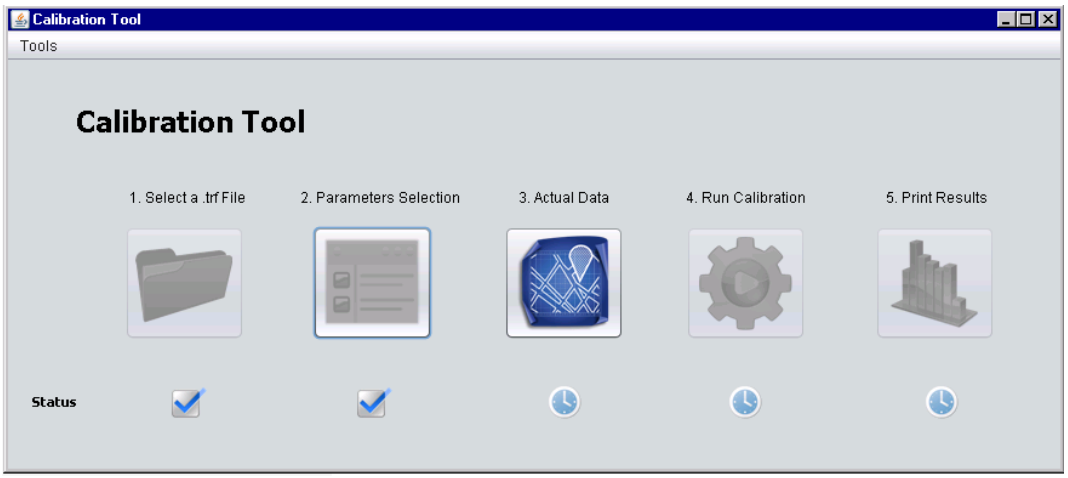

Data Editor

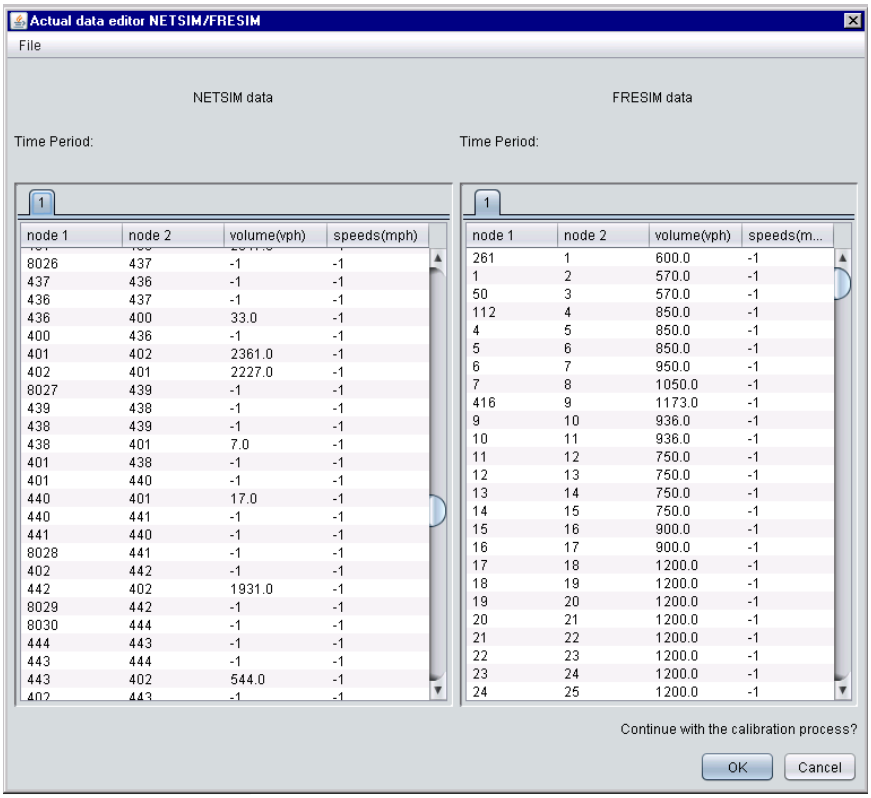

Step 4: Search of Parameters

Once the actual data is uploaded, ‘Run Calibration’ is used to execute the proposed calibration approach to find the set of parameters that minimizes the difference between actual and simulated network states.

Run Calibration

Step 5: Visualization of Results

Once the search process has determined the desired set of parameters, charts are generated to illustrate the quality of calibrated model relative to the actual data. Three sets of graphs are generated, including the GEH statistics, the ‘before’ and ‘after’ counts, and the speeds before and after the calibration. The calibrated .trf file replaces the original file.

Visualization of Results

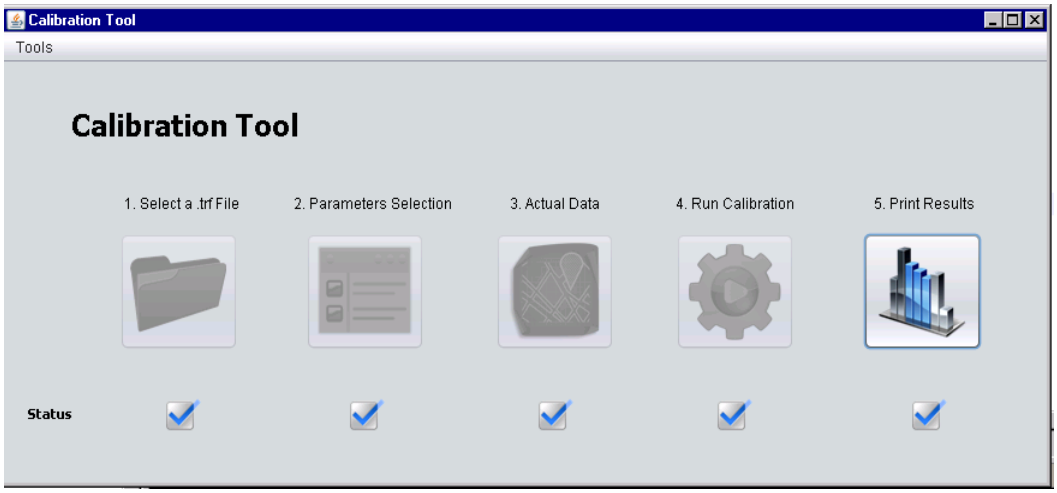

GEH Statistics

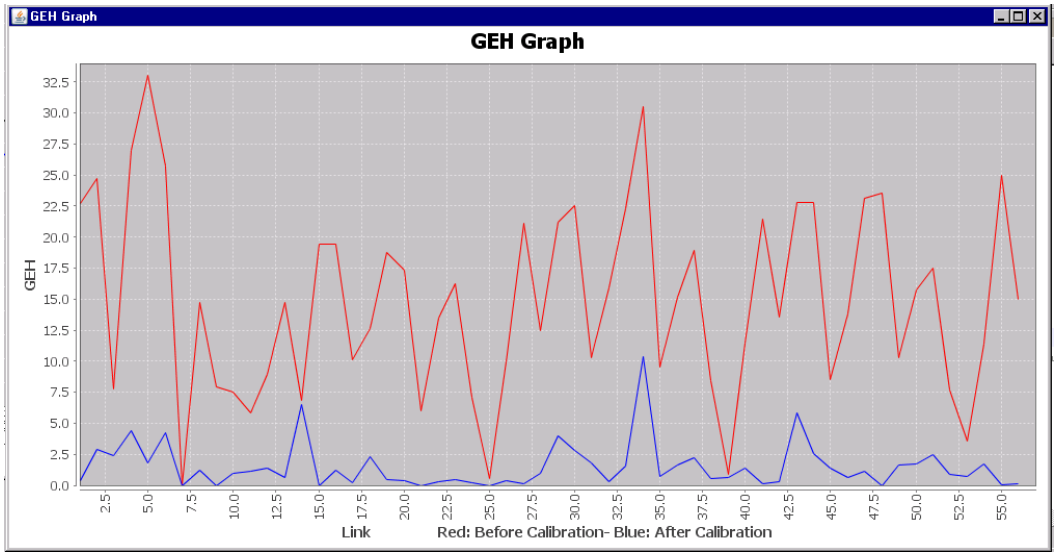

Counts Before and After Calibration

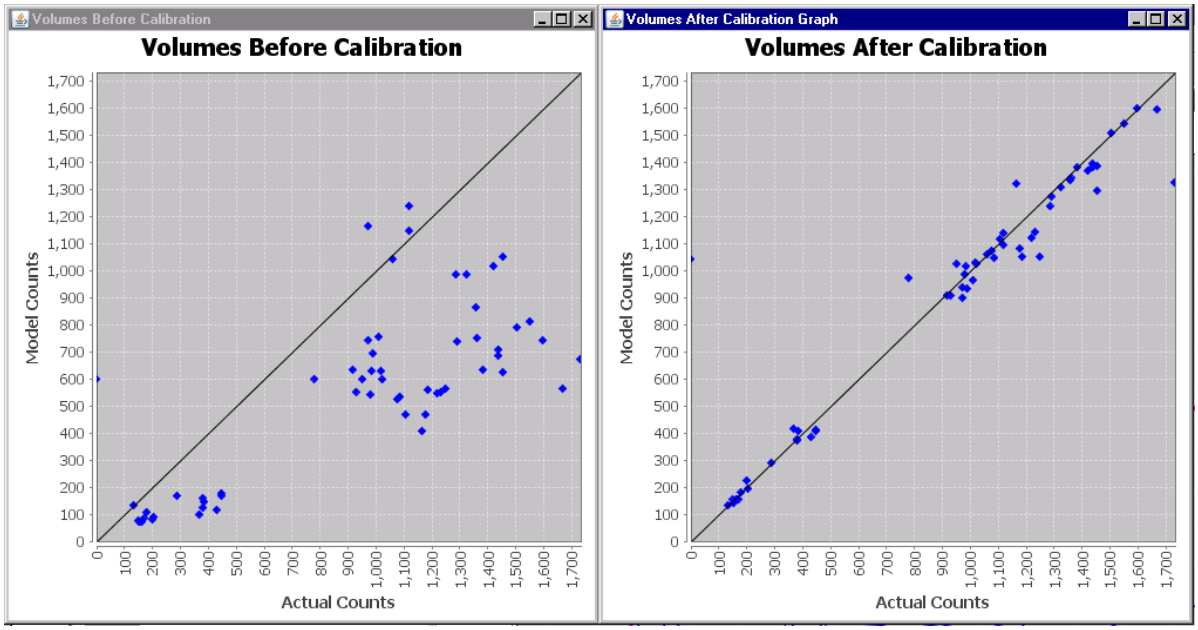

Speeds Before and After Calibration

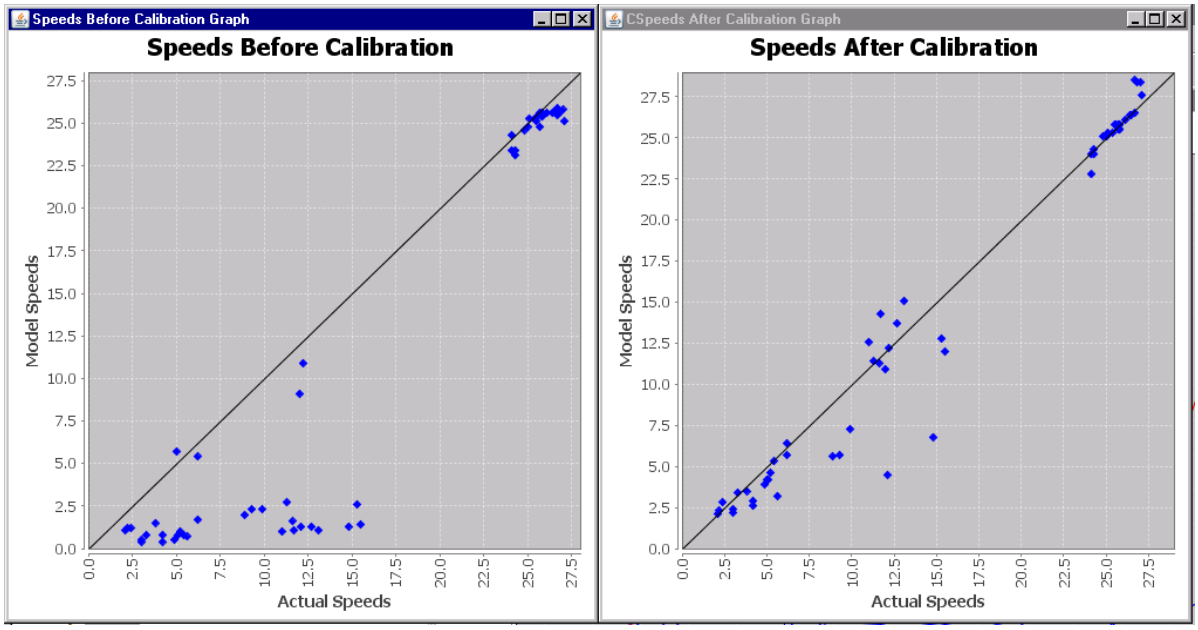

REFERENCES

Anderson, R. E., & Hicks, C. (2011). Highlights of contemporary microsimulation. Social Science Computer Review, 29(1), 3-8. doi:10.1177/0894439310370084

Balakrishna, R., Antoniou, C., Ben-Akiva, M., Koutsopoulos, H. N., & Wen, Y. (2007). Calibration of microscopic traffic simulation models: Methods and application. Transportation Research Record, (1999), 198-207. doi:10.3141/1999-21

Breski, D., Cvitanic, D., & Lovric, I. (2006). Sensitivity analysis of the CORSIM simulation model parameters; analiza osjetljivosti parametara simulacijskog modela CORSIM. Gradevinar, 58(7), 539-548.

Brockfeld, E., Kuhne, R. D., & Wagner, P. (2005). Calibration and validation of microscopic models of traffic flow. Transportation Research Record, (1934), 179-187.

Chin, D. C. (1997). Comparative study of stochastic algorithms for system optimization based on gradient approximations. Systems, Man, and Cybernetics, Part B: Cybernetics, IEEE Transactions On, 27(2), 244-249.

Cunha, A. L., Bessa Jr., J. E., & Setti, J. R. (2009). Genetic algorithm for the calibration of vehicle performance models of microscopic traffic simulators. Paper presented at the 14th Portuguese Conference on Artificial Intelligence, , 5816 LNAI 3-14. doi:10.1007/978-3-642-04686-5_1

Holm, P., Tomich, D., Sloboden, J., & Lowrance, C. (2007). Traffic analysis toolbox volume IV: Guidelines for applying CORSIM microsimulation modeling software. (No. FHWA-HOP-07-079).ITT Industries, Inc.

Hourdakis, J., Michalopoulos, P., & Kottommannil, J. (2003). Practical procedure for calibrating microscopic traffic simulation models. Transportation Research Record, (1852), 130-139.

Jha, M., Gopalan, G., Garms, A., Mahanti, B. P., Toledo, T., & Ben-Akiva, M. (2004). Development and calibration of a large-scale microscopic traffic simulation model. Paper presented at the (1876) 121-131.

Kim, K., & Rilett, L. R. (2003). Simplex-based calibration of traffic microsimulation models with intelligent transportation systems data. Paper presented at the (1855) 80-89.

Kondyli, A., Soria, I., Duret, A., & Elefteriadou, L. (2012). Sensitivity analysis of CORSIM with respect to the process of freeway flow breakdown at bottleneck locations. Simulation Modelling Practice and Theory, 22(0), 197-206. doi:10.1016/j.simpat.2011.12.008

Lee, J. (2008). Calibration of traffic simulation models using simultaneous perturbation stochastic approximation (SPSA) method extended through bayesian sampling methodology. (Ph.D., Rutgers The State University of New Jersey - New Brunswick). ProQuest Dissertations and Theses, Retrieved from http://search.proquest.com/docview/304453312?accountid=3611. (304453312).

Lee, J., & Ozbay, K. (2009). New calibration methodology for microscopic traffic simulation using enhanced simultaneous perturbation stochastic approximation approach. Transportation Research Record, (2124), 233-240. doi:10.3141/2124-23

Ma, J., Dong, H., & Zhang, H. M. (2007). Calibration of microsimulation with heuristic optimization methods. Transportation Research Record, (1999), 208-217. doi:10.3141/1999-22

Maryak, J. L., & Spall, J. C. (2005). Simultaneous perturbation optimization for efficient image restoration. Aerospace and Electronic Systems, IEEE Transactions On, 41(1), 356-361.

McTrans.Traffic software integrated system - corridor simulation. Retrieved 03/01, 2011, from http://mctrans.ce.ufl.edu/featured/TSIS/

Schultz, G. G., & Rilett, L. R. (2004). Analysis of distribution and calibration of car-following sensitivity parameters in microscopic traffic simulation models. Paper presented at the (1876) 41-51.

Schultz, G. G., & Rilett, L. R. (2005). Calibration of distributions of commercial motor vehicles in CORSIM. Transportation Research Record, (1934), 246-255.

Spall, J. C. (1998a). An overview of the simultaneous perturbation method for efficient optimization. Johns Hopkins APL Technical Digest, 19(4), 482 - 492.

Spall, J. C. (2003). Introduction to stochastic search and optimization : Estimation, simulation, and control. New Jersey: John Wiley & Sons, Inc.

Spall, J. C. (1995). Stochastic version of second-order (newton-raphson) optimization using only function measurements. Paper presented at the Simulation Conference Proceedings, 1995. Winter, 347-352. doi:10.1109/WSC.1995.478756

Spall, J. C. (1998b). Implementation of the simultaneous perturbation algorithm for stochastic optimization. Aerospace and Electronic Systems, IEEE Transactions On, 34(3), 817-823. doi:10.1109/7.705889

Toledo, T., Ben-Akiva, M., Darda, D., Jha, M., & Koutsopoulos, H. N. (2004). Calibration of microscopic traffic simulation models with aggregate data. Transportation Research Record, (1876), 10-19.

Kondyli, A., Soria, I., Duret, A., &Elefteriadou, L. (2012). Sensitivity analysis of CORSIM with respect to the process of freeway flow breakdown at bottleneck locations. Simulation Modelling Practice and Theory, 22(0), 197-206. doi:http://dx.doi.org/10.1016/j.simpat.2011.12.008(Kondyli et al., 2012)